Pure cross-anisotropy for geotechnical elastic potentials

Andrzej Niemunis* & Katarzyna Staszewska†

Institute of Soil Mechanics and Rock Mechanics

Karlsruhe Institute of Technology, Germany

Keywords

cross-anisotropy, transverse isotropy, inherent anisotropy, scaling of strain, hyperelasticity, response envelopes

Abstract

The pure cross-anisotropy is understood as a special scaling of strain (or stress). The scaled tensor is used as an argument in the elastic stiffness (or compliance). Such anisotropy can be overlaid on the top of any elastic stiffness, in particular on one obtained from an elastic potential with its own stress-induced anisotropy. This superposition does not violate the Second Law. The method can be also applied to other functions like plastic potentials or yield surfaces, wherever some cross-anisotropy is desired. The pure cross-anisotropy is described by the sedimentation vector and at most two constants. Scaling with more than two purely anisotropic constants is shown impossible.

The formulation was compared with experiments and alternative approaches. Static and dynamic calibration of the pure anisotropy is also discussed. Graphic representation of stiffness with the popular response envelopes requires some enhancement for anisotropy. Several examples are presented. All derivations and examples were accomplished using the algebra program Mathematica.

*Andrzej.Niemunis@kit.edu, corresponding author

†Katarzyna.Staszewska@kit.edu, on leave from the Faculty of Civil and Environmental Engineering, Gdańsk University of Technology, Poland

1 Introduction

Elastic response is an essential part of most constitutive models for soils. It is particularly important for soil dynamics, for stability analysis [2] and for material response in the range of small-strains. This range corresponds roughly to strain amplitudes of 10^{-5} for sand and 10^{-4} for clays. Under such loading soil can be much stiffer than at amplitudes of say 10^{-3}. This paper deals with small-strain elastic (incrementally linear) stiffness only. For larger amplitudes, hysteretic [23] or cumulative models [24] are necessary. Stiffness may be a function $\mathsf{E}(\boldsymbol{\sigma})$ of stress (or strain) but it interrelates rates (or tiny increments) of stress and strain rather than stress and strain themselves.

In the elastic regime, stress should be a continuous 1-1 function $\boldsymbol{\sigma}(\boldsymbol{\varepsilon})$ of strain. Otherwise, some stress could be accumulated within a closed strain-loop, see Section 2. A thermodynamically sound elastic material model should not allow for the accumulation of stress or energy upon any closed strain loop. The energetic requirement is not trivial for soils with a barotropic (pressure-dependent) stiffness. It is well known that the barotropic elastic modulus, $E \sim p$ or $E \sim \sqrt{p}$, with a constant Poisson number ν violates the Second Law [13, 31]. In order to avoid this problem, several elastic *potentials* have been proposed in the literature, see Section 2.1. A tangential stiffness obtained from such potential is a function of stress (not only of stress invariants) and one may speak of the stress-induced anisotropy[1] ($\sigma\mathsf{A}$). It should be distinguished from the inherent cross-anisotropy[2] ($\times\mathsf{A}$), which is caused by sedimentation process and/or geological petrification (cementation) of the geostatic K_0-state. The $\times\mathsf{A}$ is independent of the current stress or strain.

Any constant cross-anisotropic stiffness $E_{ijkl}^{\times\mathsf{A}}$ can be described by five material constants, usually denoted as $E_v, E_h, \nu_h, \nu_{vh}$ and G_v, see Section 4. The main objective of this paper is to represent this stiffness in the form[3]

$$\mathsf{E}^{\times\mathsf{A}} = \mathsf{Q}^T : \mathsf{E}^{\text{iso}} : \mathsf{Q}, \tag{1}$$

wherein the elastic properties[4] are given in the isotropic stiffness E^{iso} and all pure anisotropic properties are moved to the anisotropy tensor Q. The advantage of such *separated* description follows from the fact that the same Q can be applied to any hyperelastic (and barotropic) stiffness without violating

[1] orthotropy with respect to directions of principal stresses
[2] also called transverse isotropy, polar anisotropy
[3] see Section 1.1 for notation
[4] here, Young modulus, E, and the Poisson number, ν

the Second Law. This is proven in Section 3. In other words, any basic tangential stiffness (or compliance), possibly with its own induced anisotropy, can be superposed by the pure inherent anisotropy. Here, this pure cross-anisotropy is denoted as $\times\mathsf{A}_M$, wherein M is the number of constants required for the anisotropy tensor[5] Q. Two anisotropy tensors Q, for $\times\mathsf{A}_1$ and $\times\mathsf{A}_2$, are analytically derived in Sections 5 and 6. Unfortunately, the derivation of Q for the general case $\times\mathsf{A}_3$ is not feasible as demonstrated in Section 7.

Calibration of the parameters of Q from static (cyclic) triaxial tests on samples cut in different directions or from wave velocities in different directions [8, 27] is commented in Section 8. A few remarks on experimental data for $\times\mathsf{A}$ are given in Section 9 and the advantage of $\times\mathsf{A}_2$ over $\times\mathsf{A}_1$ is demonstrated.

The graphic representation of stiffness in the form of polar response envelopes [11] is well known in the geotechnical literature. In the case of $\times\mathsf{A}$, some complications may arise from the fact that the stress rate, $\dot{\boldsymbol{\sigma}}(\boldsymbol{\sigma}^0, \dot{\boldsymbol{\varepsilon}}, \mathbf{M})$, may not be axisymmetric for the axisymmetric initial stress, $\boldsymbol{\sigma}^0$, and *co-axisymmetric*[6] strain rate, $\dot{\boldsymbol{\varepsilon}}$. The problem is caused by the dependence on the direction of sedimentation, $\mathbf{m}$, appearing here in the form of the sedimentation dyad, $\mathbf{M} = \mathbf{m}\,\mathbf{m}$. This may also cause a loss of *coaxiality*. Therefore, an enhanced graphic representation is proposed in Section 10. Some examples of extended response envelopes with $\times\mathsf{A}_2$ and polar diagrams of wave velocities are shown.

Finally, $\times\mathsf{A}_2$ is applied to stress and substituted to the Matsuoka-Nakai yield surface. The modified surface is shown graphically in Section 11. All relevant packages and notebooks for the algebra program MATHEMATICA are available from the authors.

1.1 Notation

Bold-face letters like $\boldsymbol{\sigma}$ are vectors or second rank tensors. Sans serif letters, e.g. E, are the fourth order tensors. Gibbs notation like $\dot{\boldsymbol{\sigma}} = \mathsf{E} : \dot{\boldsymbol{\varepsilon}}$ or index notation $\dot{\sigma}_{ij} = E_{ijkl}\dot{\varepsilon}_{kl}$ in the Cartesian coordinate system with usual summation over repeated (dummy) indices is used. The geotechnical sign convention is applied to $\boldsymbol{\sigma}$ and $\boldsymbol{\varepsilon}$ with compression positive. A fourth order tensor E can appear in a form of a 9×9 matrix (no Voigt 6×6 notation) denoted as $[\mathsf{E}]$. The 9×9 form facilitates some transformations in the algebra program MATHEMATICA. Similarly, $[\boldsymbol{\sigma}]$ is the 3×3 matrix obtained from the tensor $\boldsymbol{\sigma}$. The essential variables are:

[5] also called anisotropy operator in the literature [25]

[6] =axisymmetric with respect to the same symmetry axis

$\mathbf{1}, \mathsf{I}$	identity operators
$\boldsymbol{\alpha}$	direction cosines
α, β, γ	constants for $\times\mathsf{A}$
C	elastic compliance
$\boldsymbol{\delta}$	Kronecker symbol
$\{\mathbf{e}^{\star}_P, \mathbf{e}^{\star}_Q, \mathbf{e}^{\star}_R\}$	basis for a stress space
E, ν, G, K	isotropic el. constants
E	elastic stiffness
$\boldsymbol{\varepsilon}$	strain tensor
$\bar{\boldsymbol{\varepsilon}}$	modified strain tensor
$\varepsilon_a, \varepsilon_r$	axial and radial strain components
$\varepsilon_{\mathrm{vol}}, \varepsilon_q$	Roscoe strains
$\varepsilon_P, \varepsilon_Q$	isometric strains
$\boldsymbol{\Gamma}$	acoustic tensor
$\mathbf{m}$	sedimentation vector
$\mathbf{M} = \mathbf{m}\,\mathbf{m}$	sedimentation dyad
$\mathbf{n}$	direction of wave propagation
$p, q > 0$	Roscoe stress invariants
P, Q	isometric stresses
$P^{\star}, Q^{\star}, R^{\star}$	isometric coordinates for stress increments

Q	anisotropy tensor
$R = \lVert\boldsymbol{\sigma}\rVert$	stress norm
$\boldsymbol{\sigma}$	stress tensor
$\bar{\boldsymbol{\sigma}}$	modified stress
σ_a, σ_r	axial and radial stress components
v	wave velocity
$W(\boldsymbol{\varepsilon})$	elastic energy
$\bar{W}(\boldsymbol{\sigma})$	complementary energy
$\dot{\sqcup}$	material rate of $\sqcup$
$\lVert \sqcup \rVert$	Frobenius norm of $\sqcup$
$\vec{\sqcup} = \frac{\sqcup}{\lVert\sqcup\rVert}$	normalized $\sqcup$

$\times\mathsf{A}$	pure inherent cross-anisotropy
$\sigma\mathsf{A}$	stress-induced anisotropy
$\times\mathsf{A}_M$	cross-anisotropy with M constants

2 Elastic potential

Let us consider an incrementally linear relation

$$\dot{\sigma}_{ij} = E_{ijkl}\dot{\varepsilon}_{kl} \tag{2}$$

between the stress rate $\dot{\sigma}_{ij}$ and the strain rate $\dot{\varepsilon}_{kl}$. The tangential stiffness E_{ijkl} needs not be constant. It may be a function of stress or strain but it cannot be a function of their rates. Such incrementally linear model is called hypoelastic.

Let the strain evolve along the path[7] $\varepsilon_{ij}(\tau)$, Fig. 1a. After a 180° reversal, identical negative strain increments can be applied in the opposite sequence and the strain evolves back along exactly the same path. The relation $\dot{\sigma}_{ij}(-\dot{\varepsilon}_{kl}) = -\dot{\sigma}_{ij}(\dot{\varepsilon}_{kl})$ holds due to the incremental linearity. Hence, the same stress path is followed and, eventually, the original state $\sigma_{ij}(t_0)$ is reached. The energy density, $\mathrm{d}W = \sigma_{ij}\dot{\varepsilon}_{ij}\mathrm{d}t$, is also recovered. However, if one departs from $\varepsilon_{ij}(t_0)$ upon one path and returns to $\varepsilon_{ij}(t_0)$ upon another

[7] parametrized by a time-like variable $\tau \in \{t_0, t_1\}$

path, Fig. 1b, then neither the initial stress nor the energy is in general recovered. At least, one cannot conclude such recovery from the incremental linearity (2) alone.

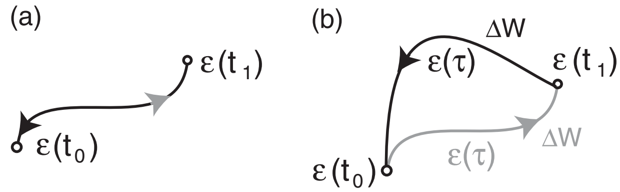

Figure 1: *Strain paths tested with incrementally linear elasticity*

In *hyperelastic* models, apart from the linear relation (2), some additional conditions must be imposed on E_{ijkl}. In isothermal elastic materials, strain is the only independent state variable, i.e. ε_{ij} alone dictates the internal elastic energy W. This dependence must be a *function* $W(\boldsymbol{\varepsilon})$, i.e. the elastic energy cannot depend on the strain path $\varepsilon_{ij}(\tau)$. The change in W upon the path from $\varepsilon^0_{ij} = \varepsilon_{ij}(t_0)$ to $\varepsilon^1_{ij} = \varepsilon_{ij}(t_1)$ is

$$\Delta W = \int \sigma_{ij} \mathrm{d}\varepsilon_{ij} = \int_{t_0}^{t_1} \sigma_{ij}(\tau)\dot{\varepsilon}_{ij}(\tau)\mathrm{d}\tau \tag{3}$$

and this ΔW is identical upon any strain path $\varepsilon_{ij}(\tau)$. If the choice of a path $\varepsilon_{ij}(\tau)$ between ε^0_{ij} and ε^1_{ij} could influence the integral ΔW, then one could input less energy upon one path, $0 \to 1$, than could be recovered on the way back, $1 \to 0$. Such gain of energy without any change of state (strain returns to ε^0_{ij}) violates the Second Law. Even if this gain occurred at the cost of thermal energy, it would be a violence of the Second Law (a perpetuum mobile of the second kind). Hence, the integral in (3) should indeed be path-independent, which implies the existence of a function $W(\boldsymbol{\varepsilon})$. Being a function, $W(\boldsymbol{\varepsilon})$ has the total differential

$$\mathrm{d}W = (\partial W/\partial \varepsilon_{ij})\mathrm{d}\varepsilon_{ij}. \tag{4}$$

From the comparison of (4) with (3) for any $\mathrm{d}\varepsilon_{ij}$, it follows that

$$\sigma_{ij} = \partial W/\partial \varepsilon_{ij}. \tag{5}$$

As a derivative of a function of strain, stress also must be a *function* $\boldsymbol{\sigma}(\boldsymbol{\varepsilon})$. Stress rate can be calculated using the chain rule, $\dot{\sigma}_{ij} = (\partial\sigma_{ij}/\partial\varepsilon_{kl})\dot{\varepsilon}_{kl}$. From the comparison with (2)

$$\dot{\sigma}_{ij} = \left[\partial^2 W/(\partial\varepsilon_{ij}\partial\varepsilon_{kl})\right]\dot{\varepsilon}_{kl}, \quad \text{follows} \quad E_{ijkl} = \partial^2 W/(\partial\varepsilon_{ij}\partial\varepsilon_{kl}). \tag{6}$$

It is evident from $(6)_2$ that E_{ijkl} must be symmetric. Note, however, that the symmetry, $E_{klij} = E_{ijkl}$, is only a necessary (but not sufficient) condition for the existence of an elastic potential. Let a symmetric stiffness $E_{klij}(\boldsymbol{\varepsilon})$ be a primary function. For the existence of $W(\boldsymbol{\varepsilon})$, also a function $\sigma_{ij}(\boldsymbol{\varepsilon})$ must exist. For the integrability

$$\int E_{ijkl}\mathrm{d}\varepsilon_{kl} \longrightarrow \sigma_{ij}(\varepsilon_{kl}), \tag{7}$$

all mixed second derivatives of $\sigma_{ij}(\varepsilon_{kl})$ must be identical

$$\partial^2\sigma_{ij}/(\partial\varepsilon_{kl}\partial\varepsilon_{rs}) = \boxed{\partial E_{ijkl}/\partial\varepsilon_{rs} = \partial E_{ijrs}/\partial\varepsilon_{kl}} = \partial^2\sigma_{ij}/(\partial\varepsilon_{rs}\partial\varepsilon_{kl}), \tag{8}$$

which is not guaranteed by the symmetry $E_{klij} = E_{ijkl}$. For example, $E_{ijkl}(\boldsymbol{\varepsilon}) = \varepsilon_{nn}\left[3K\nu\delta_{ij}\delta_{kl}/(1+\nu) + 2GI_{ijkl}\right]$ is symmetric but it is not hyperelastic because it does not satisfy the condition (8).

Functions $W(\boldsymbol{\varepsilon})$ cannot be directly measured. They are usually formulated by trial and error. An educated guess can be based on the measurements of the second derivatives E_{ijkl} $(6)_2$ at different strains. Alternatively, the complementary energy $\bar{W}(\boldsymbol{\sigma})$ may be used,

$$\bar{W} = \sigma_{ij}\varepsilon_{ij} - W \quad \text{with} \quad \varepsilon_{ij} = \partial\bar{W}/\partial\sigma_{ij} \quad \text{and} \quad E^{-1}_{ijkl} = \partial^2\bar{W}/(\partial\sigma_{ij}\partial\sigma_{kl}). \tag{9}$$

In granular materials, the main difficulty in the formulation of $W(\boldsymbol{\varepsilon})$ or $\bar{W}(\boldsymbol{\sigma})$ arises from the pressure dependence (the so-called barotropy) of the stiffness.

2.1 Geotechnical hyperelastic models

Several hyperelastic models have been proposed in the literature. A critical review can be found in [20] and more recently in [9]. It is helpful to assume the hyperelastic stiffness as a homogeneous function of stress, i.e. $\forall\lambda > 0 : \mathsf{E}(\lambda\boldsymbol{\sigma}) = \lambda^m\mathsf{E}(\boldsymbol{\sigma})$. The order m of homogeneity is usually $m \approx 0.6$ for sand and $m \approx 1$ for clays. The compliance, $\mathsf{C} = \mathsf{E}^{-1}$, is homogeneous of order $-m$, of course. It can be proven[8] that the corresponding elastic potentials, $\bar{W}(\boldsymbol{\sigma})$ and $W(\boldsymbol{\varepsilon})$, are homogeneous functions of order $2-m$ and $(2-m)/(1-m)$, respectively.

A simple hyperelasticity was proposed by Vermeer [28]. The hyperelastic potential is given explicitly,

$$\bar{W}(\boldsymbol{\sigma}) = c_1 R^{1-m/2} \tag{10}$$

with a material constant c_1. The order of homogeneity of $\mathsf{E}(\boldsymbol{\sigma})$ must be $m \neq 1$.

Borja et. al [4] proposed a hyperelastic model based on elastic potential formulated in terms of the strain invariants,

$$W(\boldsymbol{\varepsilon}) = c_3 \exp\left(\varepsilon_{\text{vol}}/c_2\right) + \left[c_4 + c_5 \exp\left(\varepsilon_{\text{vol}}/c_2\right)\right] \|\boldsymbol{\varepsilon}^*\|^2 \quad \text{with} \quad \varepsilon_{\text{vol}} = \varepsilon_{ii}, \tag{11}$$

wherein $\boldsymbol{\varepsilon}^*$ is the deviatoric part of $\boldsymbol{\varepsilon}$. In this case, the stiffness appears to be inhomogeneous in stress.

Niemunis and Cudny [20] introduced a potential for clays,

$$\begin{aligned} \bar{W}(\boldsymbol{\sigma}) &= c_6 R^2/P + c_7 R + c_8 I^{1/3} + c_9 P + c_{10} \ln(P) \\ &\text{with} \quad P = \sigma_{ii}/\sqrt{3} \quad \text{and} \quad I = \sigma_{ij}\sigma_{jk}\sigma_{ki}, \end{aligned} \tag{12}$$

that yields stiffness $\mathsf{E}(\boldsymbol{\sigma})$ with a homogeneity of order $m = 1$.

The following expression for the complementary energy was proposed for sand by Niemunis et al. [21]

$$\bar{W}(\boldsymbol{\sigma}) = c_{11} P^{c_{12}} R^{2-m-c_{12}}, \tag{13}$$

wherein $m \neq 1$ is the order of homogeneity of $\mathsf{E}(\boldsymbol{\sigma})$.

Response envelopes [11] are polar representations of stiffness at different stresses, see Section 10. They can be measured (here for medium dense sand [14, 15]) and calculated analytically, e.g. using (13). A comparison like in Fig. 2 may be used for the calibration.

[8]For this purpose, one may use $(2-m)(1-m)\bar{W}(\boldsymbol{\sigma}) = \boldsymbol{\sigma} : \frac{\partial^2 \bar{W}}{\partial \boldsymbol{\sigma} \partial \boldsymbol{\sigma}} : \boldsymbol{\sigma} = \boldsymbol{\sigma} : \mathsf{C} : \boldsymbol{\sigma}$, which is analogous to the well known Euler formula for homogeneous functions, here applied twice to $\bar{W}(\boldsymbol{\sigma})$. The homogeneity of $\bar{W}(\boldsymbol{\sigma})$ of order $2-m$ is sufficient (but not necessary) for the homogeneity of order m in $\mathsf{E}(\boldsymbol{\sigma})$. After adding a constant to $\bar{W}(\boldsymbol{\sigma})$, the homogeneity of $\bar{W}(\boldsymbol{\sigma})$ is lost but homogeneity of $\mathsf{E}(\boldsymbol{\sigma})$ is preserved.

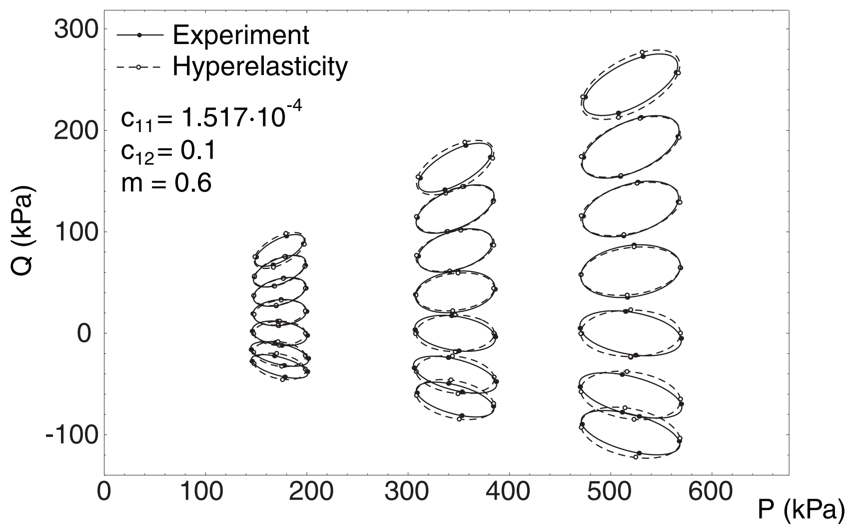

Figure 2: *Comparison between response envelopes of the experiments for medium dense sand [15] and theoretical response envelopes from (13): The presence of $\sigma\mathsf{A}$ is evident and no $\times\mathsf{A}$ is needed.*

Selected terms from (12) and (13) have been recently combined for kaolin by Gehring [9] into

$$\bar{W}(\boldsymbol{\sigma}) = c_{11}P^{c_{12}}R^{2-m-c_{12}} + c_{13}P\ln(P). \tag{14}$$

This potential is suitable for cohesive materials because the second summand removes the singularity of C at $m = 1$. Experimental (for kaolin [9]) response envelopes are compared with the theoretical ones obtained with (14), Fig. 3. A strong inherent anisotropy was caused by K_0-consolidation of kaolin. The required anisotropy tensor Q given in (27) is described in Section 5.

The proposed superposition of $\sigma\mathsf{A}$ and $\times\mathsf{A}$ is a convenient alternative to a direct postulation of $W(\boldsymbol{\sigma}, \mathbf{M})$ with the sedimentation dyad $\mathbf{M} = \mathbf{m}\,\mathbf{m}$ as an additional argument. For example such function

$$\bar{W}(\boldsymbol{\sigma}, \mathbf{M}) = \bar{R}^{1-m/2} \quad \text{with} \quad \bar{R} = c_{14}R + c_{15}M_{ab}\sigma_{bc}\sigma_{ca} \tag{15}$$

was proposed by Cudny and Staszewska [7] for $m \neq 1$. Similar approach related to the microscopic description has been recently proposed by Amorosi, Houlsby and Rollo [1, 12].

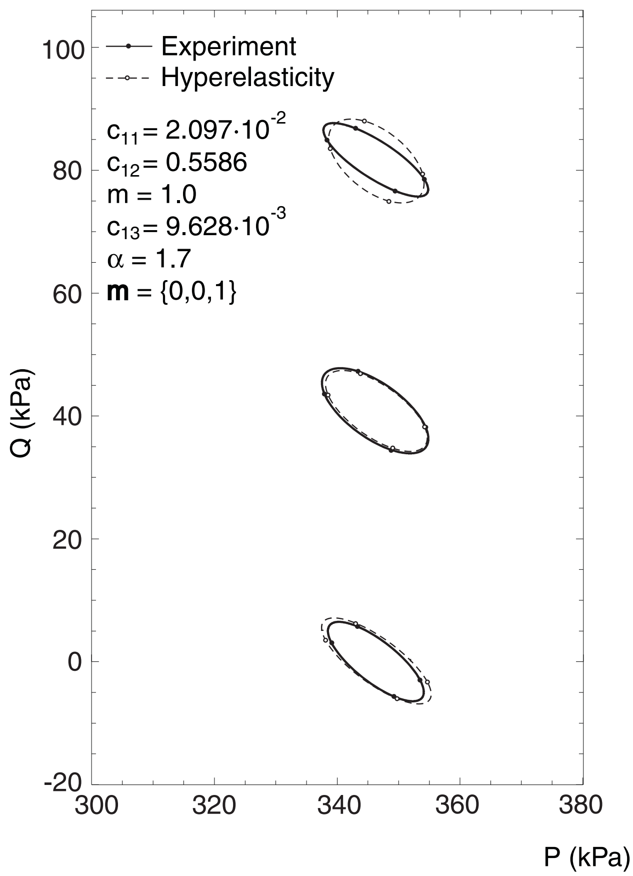

Figure 3: *Comparison between response envelopes of the experiments on kaolin [9] and theoretical response envelopes from (14): The effect of* $\times\mathsf{A}_1$ *from Section 5 is essential.*

Instead of using an explicit potential $\bar{W}(\boldsymbol{\sigma})$, Boyce [5] postulated a 1-1 homogeneous function $\boldsymbol{\varepsilon}(\boldsymbol{\sigma})$ of order $1-m$. In this case, existence of the complementary elastic potential $\bar{W}(\boldsymbol{\sigma})$ should be proven. For such formulation, the superposition described in the next sections can also be applied using identical tensor Q.

3 Anisotropy tensor Q

Stiffness E_{ijmn} and a family of transformations $E'_{ijmn} = \alpha_{ik}\alpha_{jl}\alpha_{mr}\alpha_{ns}E_{klrs}$ with directional cosines α_{ij} build a symmetry group, if the components of stiffness are preserved, that is, if $E'_{ijmn} = E_{ijmn}$. For an isotropic stiffness E^{iso}_{ijmn}, it is true for any α_{ij}. For an inherent cross-anisotropic stiffness $E^{\times\mathsf{A}}_{ijmn}$ with sedimentation direction $\mathbf{m} = \{0, 0, 1\}$, α_{ij} corresponds to an arbitrary rotation[9] around $\mathbf{m}$ by angle ψ,

$$[\boldsymbol{\alpha}] = \begin{bmatrix} \cos\psi & \sin\psi & 0 \\ -\sin\psi & \cos\psi & 0 \\ 0 & 0 & 1 \end{bmatrix}. \tag{16}$$

In this paper, the pure inherent cross-anisotropy $\times\mathsf{A}$ in a form of tensor Q is proposed. It is a function of $\mathbf{m}$ and some constants. This $\times\mathsf{A}$ can be "added" to any stiffness, e.g. to one obtained from a potential $W(\boldsymbol{\varepsilon})$ or $\bar{W}(\boldsymbol{\sigma})$ with its own $\sigma\mathsf{A}$, see Section 2.1. The constants in Q can be determined from the transformation

$$E^{\times\mathsf{A}}_{ijkl} = Q_{abij} E^{\text{iso}}_{abcd} Q_{cdkl} \tag{17}$$

of the isotropic stiffness E^{iso}_{abcd} to the desired $E^{\times\mathsf{A}}_{ijkl}$. Tensor Q should scale any stiffness in a similar manner. All components of Q are independent of ε_{ij}, E and ν, and hence, Q stores the pure anisotropy.

Let us apply Q to the strain, $\bar{\varepsilon}_{ij} = Q_{ijkl}\varepsilon_{kl}$, and then substitute $\bar{\varepsilon}_{ij}$ into an elastic potential $W(\bar{\boldsymbol{\varepsilon}})$. Differentiating $W(\bar{\boldsymbol{\varepsilon}})$ with respect to ε_{ij} and using the chain rule, one obtains the stiffness with the combined effect of $\sigma\mathsf{A}$ and $\times\mathsf{A}$,

$$E^{\times\mathsf{A}+\sigma\mathsf{A}}_{ijkl} = \frac{\partial^2 W(\bar{\boldsymbol{\varepsilon}})}{\partial\varepsilon_{ij}\partial\varepsilon_{kl}} = \frac{\partial^2 W(\bar{\boldsymbol{\varepsilon}})}{\partial\bar{\varepsilon}_{ab}\partial\bar{\varepsilon}_{cd}} \frac{\partial\bar{\varepsilon}_{ab}}{\partial\varepsilon_{ij}} \frac{\partial\bar{\varepsilon}_{cd}}{\partial\varepsilon_{kl}} = E^{\sigma\mathsf{A}}_{abcd} Q_{abij} Q_{cdkl}, \tag{18}$$

wherein $E^{\sigma\mathsf{A}}_{abcd}$ is the stiffness with $\sigma\mathsf{A}$ only. Note that *deviations* from isotropy are superposed and hence, the symmetry group is restricted rather than extended. Tensors Q have relatively simple forms for $\times\mathsf{A}_1$ and $\times\mathsf{A}_2$ with the major symmetry, $Q_{ijab} = Q_{abij}$, see Sections 5 and 6.

Inverting both sides of (17), one may use Q^{-1}_{ijkl} for the compliance[10],

$$C^{\times\mathsf{A}}_{ijkl} = Q^{-1}_{abij} C^{\text{iso}}_{abcd} Q^{-1}_{cdkl}. \tag{19}$$

The same Q^{-1}_{ijkl} can be applied to stress, $\bar{\sigma}_{ij} = Q^{-1}_{ijkl}\sigma_{kl}$, and the modified stress $\bar{\sigma}_{ij}$ can be substituted into the given complementary potential $\bar{W}(\bar{\boldsymbol{\sigma}})$.

[9] This family of α_{ij} can be completed by rotations or reflection that reverse the sense of x_3 axis.

[10] The tensors Q proposed for $\times\mathsf{A}_1$ and $\times\mathsf{A}_2$ can be analytically inverted, see Section 6.

Differentiating with the chain rule, one obtains the compliance with superposed effects of $\sigma\mathsf{A}$ and $\times\mathsf{A}$,

$$C_{ijkl}^{\times\mathsf{A}+\sigma\mathsf{A}} = \frac{\partial^2 \bar{W}(\bar{\boldsymbol{\sigma}})}{\partial\sigma_{ij}\partial\sigma_{kl}} = \frac{\partial^2 W(\bar{\boldsymbol{\sigma}})}{\partial\bar{\sigma}_{ab}\bar{\sigma}_{cd}} \frac{\partial\bar{\sigma}_{ab}}{\partial\sigma_{ij}} \frac{\partial\bar{\sigma}_{cd}}{\partial\sigma_{kl}} = C_{abcd}^{\sigma\mathsf{A}} Q_{abij}^{-1} Q_{cdkl}^{-1}, \tag{20}$$

wherein $C_{abcd}^{\sigma\mathsf{A}}$ is the compliance with $\sigma\mathsf{A}$ only.

Summing up, the most important advantage of the pure anisotropy is the fact that it can be "added" a posteriori to any hyperelastic stiffness $\mathsf{E}^{\sigma\mathsf{A}}$ or compliance[11] $\mathsf{C}^{\sigma\mathsf{A}}$ without violating the Second Law. Moreover, a fairly easy implementation of Q to existing constitutive models can be expected. Tensor Q can be interpreted as a modifier of the strain tensor[12] $\varepsilon_{ij} = -\frac{1}{2}\left(\partial u_i/\partial x_j + \partial u_j/\partial x_i\right)$. In the case of $\times\mathsf{A}_1$, a special form of Q derived in Section 5 allows to interpret this strain transformation as scaling of the displacements u_i and the coordinates x_i. This has already been observed by Lodge [17] and used for scaling of boundary value problems. Contrarily to the current approach, Lodge started by scaling of displacements $\mathbf{u}$ and coordinates $\mathbf{x}$, which imposes an unnecessary constraint on the scaling of strains $\boldsymbol{\varepsilon}$. For example, the anisotropy $\times\mathsf{A}_2$ cannot be squeezed into the class of anisotropic elastic solids discussed in [17], see Section 6.

A different cross-anisotropic scaling was proposed by Osinov and Wu [25]. They applied a diagonal fourth rank tensor P to the resulting hypoplastic *stress rate* $\dot{\boldsymbol{\sigma}}$ as follows

$$\dot{\boldsymbol{\sigma}} = \mathsf{P} : (\mathsf{E} : \dot{\boldsymbol{\varepsilon}} + \mathbf{N}\|\dot{\boldsymbol{\varepsilon}}\|)\,. \tag{21}$$

Our tensor Q could be applied to $\boldsymbol{\sigma}$, i.e. to the argument in $\mathsf{E}(\boldsymbol{\sigma})$ in (21). The thermodynamic aspects of $\mathsf{P} : \mathsf{E}$ were ignored in [25].

4 Cross-anisotropic constant stiffness

It is well known that a constant (stress-independent) cross-anisotropic elastic stiffness (22) requires five material constants, $E_v, E_h, \nu_h, \nu_{vh}$ and G_v. The vertical coordinate is x_v (=direction of sedimentation) and the horizontal coordinate is x_h, Fig. 4. These material constants will be separated into two

[11]or a priori to the strain or stress tensor

[12]before it is substituted into a strain potential of interest

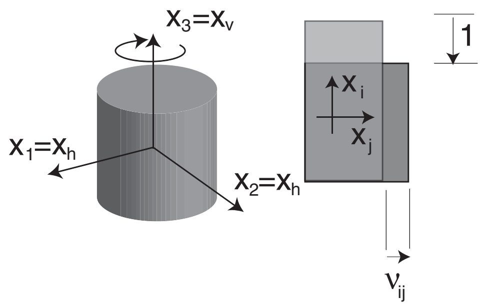

Figure 4: *Axes for cross-anisotropy and the definition of the indexed Poisson number* ν_{ij}

elastic parameters and three purely anisotropic ones. This pure anisotropy is denoted as $\times\mathsf{A}_3$. For $x_3 = x_v$, i.e. for the sedimentation direction $\mathbf{m} = \{0, 0, 1\}$, equation $\dot{\sigma}_{ij} = E^{\times\mathsf{A3}}_{ijkl}\dot{\varepsilon}_{kl}$ has the matrix form

$$\left\{ \begin{array}{c} \dot{\sigma}_{11} \\ \dot{\sigma}_{22} \\ \dot{\sigma}_{33} \\ \dot{\sigma}_{12} \\ \dot{\sigma}_{21} \\ \dot{\sigma}_{13} \\ \dot{\sigma}_{31} \\ \dot{\sigma}_{23} \\ \dot{\sigma}_{32} \end{array} \right\} = \left[\begin{array}{ccccccccc} E_h\kappa_{hh} & E_h\kappa_{hv} & E_h\kappa_{vh} & & & & & & \\ E_h\kappa_{hv} & E_h\kappa_{hh} & E_h\kappa_{vh} & & & & & & \\ E_h\kappa_{vh} & E_h\kappa_{vh} & \kappa E_v(1-\nu_h^2) & & & & & & \\ & & & G_h & G_h & & & & \\ & & & G_h & G_h & & & & \\ & & & & & G_v & G_v & & \\ & & & & & G_v & G_v & & \\ & & & & & & & G_v & G_v \\ & & & & & & & G_v & G_v \end{array} \right] \cdot \left\{ \begin{array}{c} \dot{\varepsilon}_{11} \\ \dot{\varepsilon}_{22} \\ \dot{\varepsilon}_{33} \\ \dot{\varepsilon}_{12} \\ \dot{\varepsilon}_{21} \\ \dot{\varepsilon}_{13} \\ \dot{\varepsilon}_{31} \\ \dot{\varepsilon}_{23} \\ \dot{\varepsilon}_{32} \end{array} \right\} \qquad (22)$$

wherein
$\kappa_{hh} = (1 - \nu_{hv}\nu_{vh})\,\kappa$,
$\kappa_{hv} = (\nu_h + \nu_{hv}\nu_{vh})\,\kappa$,
$\kappa_{vh} = (\nu_{vh} + \nu_h\nu_{vh})\,\kappa$ and
$\kappa = 1/\left(1 - \nu_h^2 - 2\nu_{hv}\nu_{vh} - 2\nu_h\nu_{hv}\nu_{vh}\right)$ with $\nu_h = \nu_{hh}$.
The elastic Young moduli along x_h and x_v are E_h and E_v, respectively. Shear modulus in horizontal plane is $G_h = E_h/(2(1+\nu_h))$ and from symmetry follows

$$\nu_{vh}/E_v = \nu_{hv}/E_h. \qquad (23)$$

Stability of the material behaviour requires elastic stiffness matrix to be positive-definite. This implies the following conditions on the material constants

$$E_i, G_i, \kappa > 0 \quad \text{and} \quad (\nu_{ij})^2 < E_i/E_j \quad \text{with} \quad i, j = v, h. \qquad (24)$$

The pure anisotropy tensor Q corresponding to $\times\mathsf{A}_3$ is discussed in Section 7 after the presentation of $\times\mathsf{A}_1$ and $\times\mathsf{A}_2$ in Sections 5 and 6.

5 Anisotropy tensor for $\times\mathsf{A}_1$

A three-constant elastic cross-anisotropic stiffness has been proposed by Graham and Houlsby [10] using the anisotropy parameter α in the following relations

$$\alpha = \frac{G_h}{G_v} = \sqrt{\frac{E_h}{E_v}} = \frac{\nu_h}{\nu_{vh}} \quad \overset{\text{by (23)}}{=} \frac{\nu_{hv}}{\nu_h}. \tag{25}$$

The single parameter α relates the material constants in the horizontal, $\sqcup_h$, and in the vertical (parallel to sedimentation), $\sqcup_v$, direction. The representation of stiffness for $\mathbf{m} = \{0, 0, 1\}$ with $x_3 = x_v$ is analogous to (22). In this $\times\mathsf{A}_1$ case, constant elastic stiffness matrix, $E^{\times\mathsf{A1}}_{ijkl} = Q_{abij}E^{\text{iso}}_{abcd}Q_{cdkl}$, has the form

$$\left[\mathsf{E}^{\times\mathsf{A1}}\right] = E\begin{bmatrix} \frac{\alpha^2(\nu-1)}{A} & -\frac{\alpha^2\nu}{A} & -\frac{\alpha\nu}{A} & & & & & & \\ -\frac{\alpha^2\nu}{A} & \frac{\alpha^2(\nu-1)}{A} & -\frac{\alpha\nu}{A} & & & & & & \\ -\frac{\alpha\nu}{A} & -\frac{\alpha\nu}{A} & \frac{\nu-1}{A} & & & & & & \\ & & & \frac{\alpha^2}{B} & \frac{\alpha^2}{B} & & & & \\ & & & \frac{\alpha^2}{B} & \frac{\alpha^2}{B} & & & & \\ & & & & & \frac{\alpha}{B} & \frac{\alpha}{B} & & \\ & & & & & \frac{\alpha}{B} & \frac{\alpha}{B} & & \\ & & & & & & & \frac{\alpha}{B} & \frac{\alpha}{B} \\ & & & & & & & \frac{\alpha}{B} & \frac{\alpha}{B} \end{bmatrix}, \tag{26}$$

wherein $A = 2\nu^2 + \nu - 1$ and $B = 2(\nu + 1)$. The total number of independent material constants is reduced from five to three: $E = E_v, \nu = \nu_h$ and α. Two constants describe the isotropic elasticity and just one pertains to the pure anisotropy, and hence the notation $\times\mathsf{A}_1$.

Separation of the material constants is essential. Conversion of the isotropic stiffness E^{iso} into $\times\mathsf{A}_1$ has been only mentioned in [10] without giving an explicit form. Anisotropy tensor Q has been recently derived in [21], viz.

$$\mathsf{E}^{\times\mathsf{A1}} = \mathsf{Q} : \mathsf{E}^{\text{iso}} : \mathsf{Q} \quad \text{with} \quad Q_{ijkl} = \mu_{ik}\mu_{jl} \quad \text{and} \quad \mu_{ij} = \sqrt{\alpha}\delta_{ij} + (1 - \sqrt{\alpha})m_i m_j. \tag{27}$$

Tensor Q for $\times\mathsf{A}_1$ depends on $\mathbf{m}$ and α only. In the special case of $\alpha = 1$, the anisotropy tensor is reduced to identity tensor $\delta_{ik}\delta_{jl}$. Due to the symmetry $\mu_{ij} = \mu_{ji}$, the major symmetry

$$Q_{ijkl} = \mu_{ik}\mu_{jl} = \mu_{ki}\mu_{lj} = Q_{klij} \quad \text{or} \quad \mathsf{Q}^T = \mathsf{Q} \tag{28}$$

holds. Note that μ_{ij} transforms ε_{kl} into $\bar{\varepsilon}_{ij}$ analogously as the directional cosines α_{ij} do, i.e. $\bar{\varepsilon}_{ij} = \mu_{ik}\mu_{il}\varepsilon_{kl}$, see Section 3. Hence, μ_{ij} could be used to scale the displacements u_i or the coordinate axes x_i.

The stability conditions (24) can be simplified for (25) as

$$\alpha, E > 0 \quad \text{and} \quad -1 < \nu < 0.5. \tag{29}$$

Even the simplest version $\times\mathsf{A}_1$ is reported to work well for geomaterials [9, 10, 19].

6 Anisotropy tensor for $\times\mathsf{A}_2$

It is argued [8, 19] that $\times\mathsf{A}_1$ is overly restrictive. Therefore, an $\times\mathsf{A}_2$ with two anisotropy constants, α and β, is proposed. These constants provide more flexibility for modelling of pure anisotropy. For $\beta = 1$, the $\times\mathsf{A}_1$ is recovered and for $\alpha = \beta = 1$, the tensor Q_{ijkl} is reduced to the identity. The new parameter β is added to (25) as an exponent,

$$\alpha = \frac{G_h}{G_v} = \left(\frac{E_h}{E_v}\right)^{\beta/2} = \left(\frac{\nu_h}{\nu_{vh}}\right)^{\beta} \quad \overset{\text{by (23)}}{=} \left(\frac{\nu_{hv}}{\nu_h}\right)^{\beta}. \tag{30}$$

Two isotropic elastic parameters, $E = E_v$ and $\nu = \nu_h$, are supplemented by two anisotropy constants, α and β. For such $\times\mathsf{A}_2$, an anisotropy tensor Q_{ijkl} must be found. If applied to constant isotropic elasticity, the resulting stiffness $E^{\times\mathsf{A}2}_{ijkl} = Q_{abij}E^{\text{iso}}_{abcd}Q_{cdkl}$ should be

$$\left[\mathsf{E}^{\times\mathsf{A}2}\right] = E \begin{bmatrix} \frac{\Omega^2(\nu-1)}{A} & -\frac{\Omega^2\nu}{A} & -\frac{\Omega\nu}{A} & & & & & & \\ -\frac{\Omega^2\nu}{A} & \frac{\Omega^2(\nu-1)}{A} & -\frac{\Omega\nu}{A} & & & & & & \\ -\frac{\Omega\nu}{A} & -\frac{\Omega\nu}{A} & \frac{\nu-1}{A} & & & & & & \\ & & & \frac{\Omega^2}{B} & \frac{\Omega^2}{B} & & & & \\ & & & \frac{\Omega^2}{B} & \frac{\Omega^2}{B} & & & & \\ & & & & & \frac{\theta}{B} & \frac{\theta}{B} & & \\ & & & & & \frac{\theta}{B} & \frac{\theta}{B} & & \\ & & & & & & & \frac{\theta}{B} & \frac{\theta}{B} \\ & & & & & & & \frac{\theta}{B} & \frac{\theta}{B} \end{bmatrix} \tag{31}$$

with the same A, B as defined in (26) and $\Omega = \alpha^{1/\beta}$, $\theta = \alpha^{2\beta-1}$.

By trial and error, the following anisotropy tensor has been found

$$Q_{ijkl} = \mu_{ik}\mu_{jl} + cI_{ijkl} \quad \text{with} \quad \mu_{ik} = a\delta_{ik} + bm_i m_k \tag{32}$$

and a, b, c are functions of the constants α and β, namely corrected 2.01.2022

$$\begin{aligned} a &= -\sqrt{\alpha^{\frac{2}{\beta}}\left(\left(\sqrt{\alpha}-1\right)^2 + 2\alpha^{\frac{1}{\beta}-\frac{1}{2}} + (\alpha-3)\alpha^{\frac{1}{\beta}}\right)/d}, \\ b &= -\alpha^{-\frac{1}{\beta}} a\left(\alpha + \sqrt{\alpha} - \alpha^{\frac{1}{\beta}+\frac{1}{2}} + \alpha^{\frac{1}{\beta}+1} - 2\alpha^{\frac{1}{\beta}}\right)/(\alpha-1), \\ c &= \alpha^{\frac{1}{\beta}-\frac{1}{2}}\left(\alpha - \alpha^{\frac{1}{\beta}}\right)\left(\sqrt{\alpha} + \alpha^{\frac{1}{\beta}+\frac{1}{2}} + 2\alpha^{\frac{1}{\beta}}\right)/d \quad \text{with} \qquad (33) \\ d &= \alpha + (\alpha-4)\alpha^{\frac{2}{\beta}} + 2\alpha^{\frac{1}{\beta}+1}. \qquad (34) \end{aligned}$$

The major symmetry $Q_{ijkl} = Q_{klij}$ is preserved due to symmetry $\mu_{ik} = \mu_{ki}$ given in (32). For $\mathbf{m} = \{0, 0, 1\}$, tensor Q_{ijkl} can be represented as a diagonal matrix and easily[13] inverted to Q^{-1}_{ijkl}. Otherwise, the analytical inversion requires diagonalization[14]. The new exponent β does not affect the stability condition (29). Assuming $\beta = 1$ in (30), the $\times\mathsf{A}_1$ given in (25) is recovered.

The improved flexibility of $\times\mathsf{A}_2$ goes at the expense of more complex calibration. One possibility is to assume the value of β from the literature, see Section 9.

The class of anisotropic elastic solids proposed by Lodge [17] was based on individual scaling of displacements and coordinates. This led to $\bar{\varepsilon}_{ij} = a_{ir}b_{js}\varepsilon_{rs}$. Our relation $\bar{\varepsilon}_{ij} = Q_{ijrs}\varepsilon_{rs}$ with Q_{ijrs} from (32) cannot be brought to the same form. This fact can be demonstrated using the transposition $U_{ikjl} = Q_{ijkl}$. There are two non-zero eigenvalues of U, which precludes U from being a dyad.

7 No pure anisotropy tensor for $\times\mathsf{A}_3$

Boehler and Sawczuk [3] formulated the following general representation of isotropic tensorial function of two arguments

$$\mathbf{F}(\boldsymbol{\varepsilon}, \mathbf{M}) = f_0\mathbf{1} + f_1\mathbf{M} + f_2\boldsymbol{\varepsilon} + f_3(\boldsymbol{\varepsilon}\cdot\mathbf{M} + \mathbf{M}\cdot\boldsymbol{\varepsilon}) + f_4\boldsymbol{\varepsilon}^2 + f_5(\boldsymbol{\varepsilon}^2\cdot\mathbf{M} + \mathbf{M}\cdot\boldsymbol{\varepsilon}^2) \tag{35}$$

[13] by replacing α with $1/\alpha$

[14] The diagonalization can be performed using the Hausholder reflection matrix, $H_{ij} = \delta_{ij} - 2h_i h_j$ with $\mathbf{h} = (\mathbf{e}_3 - \mathbf{m})^{\rightarrow}$. In the diagonal form, the anisotropy tensor, $Q^{\text{diag}}_{abcd} = Q_{ijkl}H_{ai}H_{bj}H_{ck}H_{dl}$, can be easily inverted and then reflected back to the initial coordinate system.

for $\mathbf{M} = \mathbf{m}\,\mathbf{m}$ being the dyad of sedimentation. In such case, $\mathbf{M} = \mathbf{M} \cdot \mathbf{M}$ and $\mathrm{tr}\,\mathbf{M} = 1$ is the only non-zero eigenvalue. The scalars f_i in (35) are functions of the following invariants

$$\mathrm{tr}\,(\boldsymbol{\varepsilon}), \mathrm{tr}\,(\boldsymbol{\varepsilon}^2), \mathrm{tr}\,(\boldsymbol{\varepsilon}^3), \mathrm{tr}\,(\mathbf{M} \cdot \boldsymbol{\varepsilon}), \mathrm{tr}\,(\mathbf{M} \cdot \boldsymbol{\varepsilon}^2). \tag{36}$$

We need $\bar{\boldsymbol{\varepsilon}} = \mathbf{F}(\boldsymbol{\varepsilon}, \mathbf{M})$ to be linear with respect to $\boldsymbol{\varepsilon}$ because $\mathsf{Q} = \partial \bar{\boldsymbol{\varepsilon}} / \partial \boldsymbol{\varepsilon}$ should be independent of $\boldsymbol{\varepsilon}$. Hence, (35) can be reduced to the following *bilinear* function

$$\mathbf{F}(\boldsymbol{\varepsilon}, \mathbf{M}) = f_0 \mathbf{1} + f_1 \mathbf{M} + f_2 \boldsymbol{\varepsilon} + f_3 (\boldsymbol{\varepsilon} \cdot \mathbf{M} + \mathbf{M} \cdot \boldsymbol{\varepsilon}), \tag{37}$$

wherein only f_0 and f_1 may depend on invariants $\mathrm{tr}\,\boldsymbol{\varepsilon}$ and $\mathrm{tr}\,(\mathbf{M} \cdot \boldsymbol{\varepsilon})$, i.e.

$$\begin{aligned} \mathbf{F}(\boldsymbol{\varepsilon}, \mathbf{M}) = \; & C_1 \mathrm{tr}\,(\boldsymbol{\varepsilon}) \mathbf{1} + C_2 \mathrm{tr}\,(\mathbf{M} \cdot \boldsymbol{\varepsilon}) \mathbf{1} + C_3 \mathrm{tr}\,(\boldsymbol{\varepsilon}) \mathbf{M} + C_4 \mathrm{tr}\,(\mathbf{M} \cdot \boldsymbol{\varepsilon}) \mathbf{M} \\ & + 2C_5 \boldsymbol{\varepsilon} + 2C_6 (\boldsymbol{\varepsilon} \cdot \mathbf{M} + \mathbf{M} \cdot \boldsymbol{\varepsilon}) \end{aligned} \tag{38}$$

with six material constants C_i. The derivative of the stress rate function $\dot{\boldsymbol{\sigma}} = \mathbf{F}(\dot{\boldsymbol{\varepsilon}}, \mathbf{M})$ in the representation (38) leads to the linear stiffness $\mathsf{E} = \partial \dot{\boldsymbol{\sigma}} / \partial \dot{\boldsymbol{\varepsilon}}$, namely

$$\begin{aligned} E_{ijkl} \;=\; & C_1 \delta_{ij} \delta_{kl} + C_2 \delta_{ij} M_{kl} + C_3 M_{ij} \delta_{kl} + C_4 M_{ij} M_{kl} + C_5 (\delta_{ik} \delta_{jl} + \delta_{il} \delta_{jk}) + \\ & C_6 (M_{ik} \delta_{jl} + M_{il} \delta_{jk} + \delta_{ik} M_{jl} + \delta_{il} M_{jk}), \end{aligned} \tag{39}$$

wherein $C_2 = C_3$ follows from the symmetry $E_{ijkl} = E_{klij}$.

In our case, function $\bar{\boldsymbol{\varepsilon}} = \mathbf{F}(\boldsymbol{\varepsilon}, \mathbf{M})$ in the representation (38) is differentiated to $\mathsf{Q} = \partial \bar{\boldsymbol{\varepsilon}} / \partial \boldsymbol{\varepsilon}$ keeping $C_2 \neq C_3$, i.e. the tensor Q has the matrix form

$$[\mathsf{Q}] = \left[\begin{array}{ccc|cccccc} C_1 + 2C_5 & C_1 & C_1 + C_2 & & & & & & \\ C_1 & C_1 + 2C_5 & C_1 + C_2 & & & & & & \\ C_1 + C_3 & C_1 + C_3 & C_7 & & & & & & \\ \hline & & & C_5 & C_5 & & & & \\ & & & C_5 & C_5 & & & & \\ & & & & & C_8 & C_8 & & \\ & & & & & C_8 & C_8 & & \\ & & & & & & & C_8 & C_8 \\ & & & & & & & C_8 & C_8 \end{array} \right], \tag{40}$$

wherein $C_7 = C_1 + C_2 + C_3 + C_4 + 2C_5 + 4C_6$ and $C_8 = C_5 + C_6$. Of course, (40) holds for $\mathbf{m} = \{0, 0, 1\}$ only. With (40) in hand, one may attempt to find the constants C_i, for which the postulated separation

$$\mathsf{E}^{\times \mathsf{A3}} = \mathsf{Q}^T : \mathsf{E}^{\mathrm{iso}} : \mathsf{Q} \tag{41}$$

of elasticity and pure anisotropy is valid. Although the matrices $\mathsf{E}^{\times \mathsf{A3}}$ and $\mathsf{E}^{\mathrm{iso}}$ are congruent, it can be shown that the separation of elastic constants, $E = E_v, \nu = \nu_h$, and purely anisotropic constants, α, β, γ, from

$$\alpha = \frac{G_h}{G_v} = \left(\frac{E_h}{E_v}\right)^{\gamma} = \left(\frac{\nu_h}{\nu_{vh}}\right)^{\beta} \quad \overset{\text{by (23)}}{=} \left(\frac{\nu_{hv}}{\nu_h}\right)^{\frac{\gamma\beta}{\beta-\gamma}} \quad \text{with} \quad \gamma \neq \beta/2 \tag{42}$$

is not possible using Q given in (40). In order to demonstrate this fact, it is convenient to investigate the compliances, $\mathsf{C}^{\mathrm{iso}}$ and $\mathsf{C}^{\times \mathsf{A3}}$, rather than the stiffnesses, $\mathsf{E}^{\mathrm{iso}}$ and $\mathsf{E}^{\times \mathsf{A3}}$. For the special case of $E = 1$, the constant isotropic compliance matrix is

$$[\mathsf{C}^{\mathrm{iso}}] = \left[\begin{array}{ccc|cccccc} 1 & -\nu & -\nu & & & & & & \\ -\nu & 1 & -\nu & & & & & & \\ -\nu & -\nu & 1 & & & & & & \\ \hline & & & \frac{1+\nu}{2} & \frac{1+\nu}{2} & & & & \\ & & & \frac{1+\nu}{2} & \frac{1+\nu}{2} & & & & \\ & & & & & \frac{1+\nu}{2} & \frac{1+\nu}{2} & & \\ & & & & & \frac{1+\nu}{2} & \frac{1+\nu}{2} & & \\ & & & & & & & \frac{1+\nu}{2} & \frac{1+\nu}{2} \\ & & & & & & & \frac{1+\nu}{2} & \frac{1+\nu}{2} \end{array}\right] \tag{43}$$

and the cross-anisotropic elastic compliance for $\mathbf{m} = \{0, 0, 1\}$ is $[\mathsf{C}^{\times \mathsf{A3}}] =$

$$\alpha^{\frac{-1}{\gamma}} \left[\begin{array}{ccc|cccccc} 1 & -\nu & -\nu\omega & & & & & & \\ -\nu & 1 & -\nu\omega & & & & & & \\ -\nu\omega & -\nu\omega & \alpha^{\frac{1}{\gamma}} & & & & & & \\ \hline & & & \frac{\nu+1}{2} & \frac{\nu+1}{2} & & & & \\ & & & \frac{\nu+1}{2} & \frac{\nu+1}{2} & & & & \\ & & & & & \frac{1}{2}\alpha(\nu+1) & \frac{1}{2}\alpha(\nu+1) & & \\ & & & & & \frac{1}{2}\alpha(\nu+1) & \frac{1}{2}\alpha(\nu+1) & & \\ & & & & & & & \frac{1}{2}\alpha(\nu+1) & \frac{1}{2}\alpha(\nu+1) \\ & & & & & & & \frac{1}{2}\alpha(\nu+1) & \frac{1}{2}\alpha(\nu+1) \end{array}\right], \tag{44}$$

wherein $\omega = \alpha^{-1/\beta+1/\gamma}$. The matrices, (43) and (44), should be coupled analogously to (41). Such coupling is possible, if a set of components of the inverse anisotropy matrix $[\mathsf{Q}^{-1}]$ can be found that satisfies

$$[\mathsf{C}^{\times \mathsf{A3}}] = [\mathsf{Q}^{-1}]^T \cdot [\mathsf{C}^{\mathrm{iso}}] \cdot [\mathsf{Q}^{-1}]. \tag{45}$$

The inverse matrix $[\mathsf{Q}^{-1}]$ has identical formal representation (40) as $[\mathsf{Q}]$. The uniqueness of the solution is not necessary. The following guess

$$
[\mathsf{Q}^{-1}] = \alpha^{\frac{-1}{2\gamma}} \left[\begin{array}{ccc|cccccc}
1 & & & & & & & & \\
 & 1 & & & & & & & \\
 & & \omega & & & & & & \\
\hline
 & & & \frac{1}{2} & \frac{1}{2} & & & & \\
 & & & \frac{1}{2} & \frac{1}{2} & & & & \\
 & & & & & \frac{\sqrt{\alpha}}{2} & \frac{\sqrt{\alpha}}{2} & & \\
 & & & & & \frac{\sqrt{\alpha}}{2} & \frac{\sqrt{\alpha}}{2} & & \\
 & & & & & & & \frac{\sqrt{\alpha}}{2} & \frac{\sqrt{\alpha}}{2} \\
 & & & & & & & \frac{\sqrt{\alpha}}{2} & \frac{\sqrt{\alpha}}{2}
\end{array}\right] \tag{46}
$$

nearly satisfies (45). Using $[\mathsf{Q}^{-1}]$ given in (46), the product $[\mathsf{Q}^{-1}]^T \cdot [\mathsf{C}^{\mathrm{iso}}] \cdot [\mathsf{Q}^{-1}]$ (45) is almost identical as $[\mathsf{C}^{\times \mathsf{A}3}]$ given in (44). Only one component of $[\mathsf{Q}^{-1}]^T \cdot [\mathsf{C}^{\mathrm{iso}}] \cdot [\mathsf{Q}^{-1}]$ differs from the respective component of $[\mathsf{C}^{\times \mathsf{A}3}]$. These components may be set equal, $\omega^2 = \alpha^{1/\gamma}$, which leads to $\gamma = \beta/2$ but this corresponds to the constraint imposed on the cross-anisotropy by $\times \mathsf{A}_2$, as described in Section 6.

The formal structure of $[\mathsf{Q}^{-1}]$ given in (40) with only a few independent C_i poses a strong limitation on the congruence relation. The congruence requires $[\mathsf{Q}^{-1}]$ to be a nonsingular matrix only. However, identical zero blocks in $[\mathsf{Q}^{-1}]$ from (40) and in $[\mathsf{C}^{\mathrm{iso}}]$ provide a major advantage for the determination of C_i, namely, the search for the 9×9 coupling matrix $[\mathsf{Q}^{-1}]$ can be split into two independent and smaller tasks:

1) coupling of the upper left 3×3 blocks
2) coupling of the lower right 6×6 blocks.

The solution of the second task can be taken as the lower right 6×6 block of $[\mathsf{Q}^{-1}]$ from (46). Unfortunately, the first task is less trivial. The upper left 3×3 block of $[\mathsf{C}^{\mathrm{iso}}]$ from (43) should be coupled with the upper left 3×3 block of $[\mathsf{C}^{\times \mathsf{A}3}]$ from (44) using just the upper left 3×3 block of $[\mathsf{Q}^{-1}]$ independently of the remaining components. Obeying the structure of $[\mathsf{Q}^{-1}]$ from (40), the first task takes the form

$$
\begin{bmatrix} 1 & -\nu & -\nu\omega \\ -\nu & 1 & -\nu\omega \\ -\nu\omega & -\nu\omega & \alpha^{\frac{1}{\gamma}} \end{bmatrix} = \begin{bmatrix} a & c & d \\ c & a & d \\ e & e & b \end{bmatrix} \cdot \begin{bmatrix} 1 & -\nu & -\nu \\ -\nu & 1 & -\nu \\ -\nu & -\nu & 1 \end{bmatrix} \cdot \begin{bmatrix} a & c & e \\ c & a & e \\ d & d & b \end{bmatrix}, \tag{47}
$$

from which five independent unknown components, a, b, c, d and e, should be found. It is a system of nonlinear equations. After removing duplicates, only four equations remain. For the true separation of elasticity and pure anisotropy, the unknowns a, b, c, d and e cannot depend on ν. Hence, one may compare independently free coefficients and coefficients at ν in each of four equations. This generates the following system of 8 equations with 5 independent unknowns

$$\left\{ \begin{array}{c|l} 1 & +0\nu \\ 0 & -1\nu \\ 0 & -\omega\nu \\ \alpha^{\frac{1}{\gamma}} & +0\nu \end{array} \right\} = \left\{ \begin{array}{c|l} a^2+c^2+d^2 & -2\left[ac+ad+cd\right]\nu \\ d^2+2ac & -\left[a^2+2ad+c^2+2cd\right]\nu \\ bd+ae+ce & -\left[ab+bc+ae+ce+2de\right]\nu \\ b^2+2e^2 & -\left[4be+2e^2\right]\nu \end{array} \right\}. \tag{48}$$

Using the powerful command `Reduce[]` from MATHEMATICA, one can algebraically reduce the system. This reduction leads to the constraint, $\omega^2 = \alpha^{1/\gamma}$, imposed on α, β and γ, identical as in $\times\mathsf{A}_2$ described in Section 6. Hence, the construction of the inverse anisotropy tensor Q^{-1} for $\times\mathsf{A}_3$ without constraints, i.e. preserving all pure anisotropy parameters, α, β and γ, is not possible.

If the elastic constant ν was allowed[15] to enter Q, then $\mathsf{E}^{\times\mathsf{A}3}$ given in (22) could be decomposed

$$\sqrt{\mathsf{E}^{\times\mathsf{A}3}/E_v} : (E_v\mathsf{I}) : \sqrt{\mathsf{E}^{\times\mathsf{A}3}/E_v} = \mathsf{E}^{\times\mathsf{A}3} \tag{49}$$

and $\mathsf{Q} = \sqrt{\mathsf{E}^{\times\mathsf{A}3}/E_v}$ could be interpreted[16]. Tensor $E_v\mathsf{I}$ describes the isotropic elastic stiffness for the special case with $\nu = 0$ and $E = E_v$.

8 Calibration of pure cross-anisotropy

Two methods of calibration of the $\times\mathsf{A}$ constants will be presented: *static* triaxial tests with small stress cycles applied in different directions and *dynamic* tests with different wave types propagated in different directions. In both cases, the average stress should be isotropic. Otherwise, the $\times\mathsf{A}$ must be calibrated jointly with the $\sigma\mathsf{A}$, which is much more difficult.

A combined partly dynamic and partly static, cyclic calibration should be avoided because the anisotropy of the small-strain stiffness may change with the size of the amplitude. Strain amplitudes due to wave propagation are usually much smaller than the ones from static cycles.

[15] no true separation of elasticity and pure anisotropy anymore

[16] The root of a symmetric matrix A can be found from spectral decomposition, $\sqrt{\mathsf{A}} = \mathsf{G}^T \cdot \sqrt{\mathsf{D}} \cdot \mathsf{G}$, where D is the diagonal matrix with eigenvalues of A and G contains the corresponding orthonormalized eigenvectors in rows.

8.1 Static calibration of $\times \mathsf{A}_1$

In this section, two methods to determine α, E_v and ν_h for the $\times \mathsf{A}_1$ are presented. The first one is based on two saturated, undrained triaxial tests and the second one needs two drained triaxial tests with measurement of the volume change. In isotropic elasticity, the volumetric and deviatoric behaviour can be described separately. Isochoric (at constant volume ≈ undrained [22]) stress paths are perpendicular to the hydrostatic axis. In anisotropic elasticity, the inclination

$$\eta = \dot{p}/\dot{q} = p^{\mathrm{ampl}}/q^{\mathrm{ampl}} \neq 0 \tag{50}$$

may be measured, see Fig. 5. The inclination η is different for the v-sample

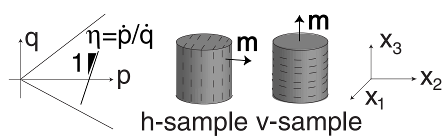

Figure 5: *Samples cut parallel (v-sample) and perpendicular (h-sample) to the direction of sedimentation* $\mathbf{m}$*: Inclination of the stress path* η *in triaxial undrained loading is shown.*

cut parallel and for the h-sample cut perpendicular to the direction of sedimentation from the same material. This can be illustrated with the results from cyclic stress tests on kaolin [29], see Fig. 6. The inclinations are inter-related by

$$\eta_v/\eta_h = -2 \tag{51}$$

and (51) holds for any $\times \mathsf{A}$. Hence η_v and η_h provide equivalent information for the calibration of α and ν, for which two conditions are required. In the coordinate system from Fig. 5 the first condition can be formulated for the v-sample

- $\eta_v = \dfrac{\dot{\sigma}_{av} + 2\dot{\sigma}_{rv}}{3(\dot{\sigma}_{av} - \dot{\sigma}_{rv})}$ with $\dot{\boldsymbol{\sigma}}_v = \mathsf{E}^v : \dot{\boldsymbol{\varepsilon}}_v$ and $\dot{\boldsymbol{\varepsilon}}_v = \mathrm{diag}(-\frac{1}{2}, -\frac{1}{2}, 1)\,.$ (52)

Assuming $E_v = 1$, the right-hand side of $(52)_2$ is a function of α and ν_h only and η_v is known. The second condition is based on the observation

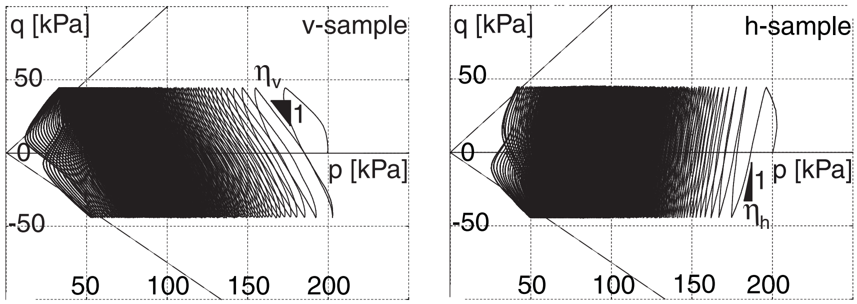

Figure 6: *Undrained triaxial tests on kaolin samples cut parallel (v-sample) and perpendicular (h-sample) to the direction of sedimentation after [29]*

that identical stress amplitudes q^{ampl} cause different strain amplitudes in the v- and h-sample. The ratio $r = \varepsilon_{av}^{\text{ampl}}/\varepsilon_{ah}^{\text{ampl}} \neq 1$ can be measured in the undrained test. Again, in the coordinate system from Fig. 5, the second condition can be expressed by three equations

$$\bullet \quad \operatorname{tr} \dot{\boldsymbol{\varepsilon}}_v = 0 \qquad \operatorname{tr} \dot{\boldsymbol{\varepsilon}}_h = 0 \qquad \dot{\varepsilon}_{av}/\dot{\varepsilon}_{ah} = r, \tag{53}$$

wherein $\dot{\boldsymbol{\varepsilon}}_v$ and $\dot{\boldsymbol{\varepsilon}}_h$ are strain rates in v-sample and h-sample caused by the same stress rate $\dot{q}_v = \dot{q}_h = \dot{\sigma}_a^{\text{tot}} - \dot{\sigma}_r^{\text{tot}} = 1$. In the conventional undrained triaxial tests with $\dot{\sigma}_r^{\text{tot}} = 0$, one may express these strain rates as

$$\dot{\boldsymbol{\varepsilon}}_v = \mathsf{C}^v : \dot{\boldsymbol{\sigma}}_v \quad \text{and} \quad \dot{\boldsymbol{\varepsilon}}_h = \mathsf{C}^h : \dot{\boldsymbol{\sigma}}_h, \tag{54}$$

wherein the *effective* stress rates

$$\dot{\boldsymbol{\sigma}}_v = \operatorname{diag}(-\dot{u}_v, -\dot{u}_v, 1 - \dot{u}_v) \quad \text{and} \quad \dot{\boldsymbol{\sigma}}_h = \operatorname{diag}(-\dot{u}_h, -\dot{u}_h, 1 - \dot{u}_h) \tag{55}$$

and the rates of pore pressures $\dot{u}_v \neq \dot{u}_h$ may be different in v- and h-samples (in spite of the same $\dot{q}$). Using the $\bullet$ conditions, one may express α and ν_h by analytical formulas, see Appendix A.

With α and ν_h in hand, one may determine the module $E_v = s\, \dot{\sigma}_{av}^{\text{tot}}/\dot{\varepsilon}_{av}$. The rates $\dot{\sigma}_{av}^{\text{tot}}$ and $\dot{\varepsilon}_{av}$ should be measured from the undrained v-sample. The scaling factor $s(\nu_h, \alpha)$ can be determined substituting into $\dot{\boldsymbol{\sigma}}_v = \mathsf{E}^v : \dot{\boldsymbol{\varepsilon}}_v$ the following relations

$$\dot{\boldsymbol{\varepsilon}}_v = \dot{\varepsilon}_{av} \operatorname{diag}(-\tfrac{1}{2}, -\tfrac{1}{2}, 1) \quad \text{and} \quad \dot{\boldsymbol{\sigma}}_v = \operatorname{diag}(-\dot{u}_v, -\dot{u}_v, \dot{\sigma}_{av}{}^{\text{tot}} - \dot{u}_v)\,. \tag{56}$$

The system $\dot{\boldsymbol{\sigma}}_v = \mathsf{E}^v : \dot{\boldsymbol{\varepsilon}}_v$ can be solved for E_v after elimination of $\dot{u}_v$. The complete solution is given in Appendix A.

Alternatively, the $\times\mathsf{A}_1$ parameter along with the elastic constants can be determined from the conventional drained triaxial tests (at $\dot{\sigma}_r = 0$). From a compresssion of a v-sample and a h-sample, one obtains $E_v = \dot{\sigma}_{av}/\dot{\varepsilon}_{av}$ and $E_h = \dot{\sigma}_{ah}/\dot{\varepsilon}_{ah}$, respectively. The measurement of volumetric and axial deformations leads to the following system

$$\begin{cases} \dot{\varepsilon}_{\mathrm{vol}\,h} & = \dot{\varepsilon}_{ah}(1 - \nu_h - \nu_{hv}) \\ \dot{\varepsilon}_{\mathrm{vol}\,v} & = \dot{\varepsilon}_{av}(1 - 2\nu_{vh}) \\ \nu_h & = \nu_{vh}\alpha = \nu_{hv}/\alpha \end{cases} \tag{57}$$

which can be solved for $\alpha, \nu_{vh}, \nu_{hv}, \nu_{hh}$, see Appendix A.

8.2 Dynamic calibration of $\times\mathsf{A}_2$

In this section only the dynamic calibration of $\times\mathsf{A}_2$ is discussed. A static calibration of β via G_v is possible but it needs a hollow-cylinder torsion test on a v-sample.

Anisotropic elastic parameters can be determined from the measurements of wave velocities (dynamic tests) in different direction of propagation $\mathbf{n}$. Using this direction, the acoustic tensor can be built

$$\Gamma_{jk} \quad = \quad n_i E_{ijkl} n_l, \tag{58}$$

wherein E is the stiffness and $\mathbf{n}$ is unit vector. The eigenvalues of Γ_{ik} are related to the velocities of different waves propagating along $\mathbf{n}$. A (phase) velocity v can be determined from the following eigenvalue problem (Christoffel equation for plane waves) [6]

$$\left(\Gamma_{jk} - \rho v^2 \delta_{jk}\right) A_k = 0_i, \tag{59}$$

wherein ρ is the mass density. Three eigenvalues ρv^2 may be obtained from $\det\left(\Gamma_{jk} - \rho v^2 \delta_{jk}\right) = 0$. They may correspond, in general, to three different waves with different velocities, all propagating along $\mathbf{n}$. The corresponding eigenvectors $\mathbf{A}$ describe the polarizations of displacement amplitudes. In the case of isotropic elasticity, it is one P-wave with $\mathbf{A}\|\mathbf{n}$ and two S-waves with $\mathbf{A} \perp \mathbf{n}$, Fig. 7. The velocities v_S and v_P are independent of $\mathbf{n}$.

In a cross-anisotropic medium with $\mathsf{E}^{\times \mathsf{A}2}$, the velocities of propagation and the polarization directions depend on the anisotropy parameters, α and

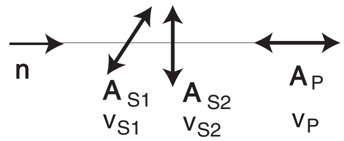

Figure 7: *Direction of propagation* **n** *with two shear waves,* v_{S1} *and* v_{S2}*, and one pressure wave,* v_P*, for isotropic elasticity*

β, and on the angle between **n** and **m**. The explicit expressions for Γ_{ik} in the case of any **n** and $\mathbf{m} = \{0, 0, 1\}$ are given in Appendix B. We examine two directions of propagation, $\mathbf{n} \| \mathbf{m}$ (index v) and $\mathbf{n} \perp \mathbf{m}$ (index h) with $\mathbf{m} = \{0, 0, 1\}$, Fig. 8. For such **n**, the polarization **A** can be either perpendicular

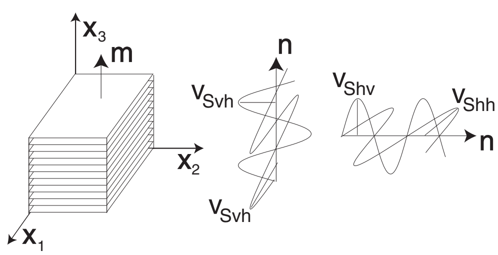

Figure 8: *Anisotropy due to sedimentation along the* x_3 *axis: Polarization of different S-waves is shown.*

or parallel to **n**. The respective eigenvalues are denoted as ρv_{Sij}^2 and ρv_{Pij}^2, wherein i is the direction of propagation and j is the direction of polarization, both taking the values h or v. The velocities for $\times \mathsf{A}_2$ can be easily found as the eigenvalues of tensors given in (72) in Appendix B

$$
\begin{aligned}
\rho v_{Shh}^2 &= \frac{E\Omega^2}{B}, \qquad \rho v_{Shv}^2 = \rho v_{Svh}^2 = \frac{E\theta}{B}, \\
\rho v_{Phh}^2 &= \frac{E\Omega^2(\nu - 1)}{A}, \qquad \rho v_{Pvv}^2 = \frac{E(\nu - 1)}{A}
\end{aligned}
\tag{60}
$$

with $A = 2\nu^2 + \nu - 1$, $B = 2(\nu + 1)$, $\Omega = \alpha^{1/\beta}$ and $\theta = \alpha^{2\beta - 1}$.

Both parameters, α and β, can be calibrated from vertical and horizontal waves[17] alone, using (60), see Fig. 9.

[17]This can be done in triaxial apparatus using bender elements installed on the end-

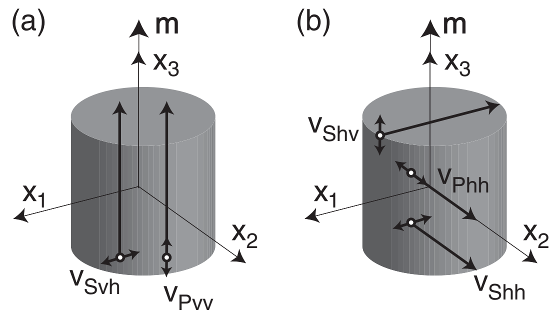

Figure 9: *Set-up of bender elements for the determination of* $\times\mathsf{A}_2$ *parameters: a) waves with vertical propagation b) waves with horizontal propagation*

Four independent wave velocities, $v_{Pvv}, v_{Phh}, v_{Shh}$ and $v_{Svh} = v_{Shv}$, can be measured and (60) can be solved for two pure anisotropic parameters

$$\alpha = \frac{v_{Shh}^2}{v_{Svh}^2}, \qquad \beta = \frac{2\ln\left(v_{Shh}^2/v_{Svh}^2\right)}{\ln\left(v_{Phh}^2/v_{Pvv}^2\right)} \tag{61}$$

and two elastic parameters, $E = E_v$ and $\nu = \nu_h$,

$$E_v = \rho v_{Pvv}^2\left(1 + \frac{4v_{Shh}^2}{v_{Phh}^2} + \frac{v_{Phh}^2}{v_{Shh}^2 - v_{Phh}^2}\right), \nu_h = 1 + \frac{v_{Phh}^2}{2(v_{Shh}^2 - v_{Phh}^2)}. \tag{62}$$

Determination of all five parameters for the stiffness (22) requires additionally a wave velocity in an inclined direction $\mathbf{n}$, say for $\mathbf{n}\cdot\mathbf{m} = 1/\sqrt{2}$ [8,27].

9 Tests of $\times\mathsf{A}$

Recently, Mašín and Rott [19] have reviewed numerous experiments on sedimentary clays. They concluded that, using the nomenclature of (42), most clays need $\gamma > 1/2$, which can be covered by $\times\mathsf{A}_2$ or $\times\mathsf{A}_3$ but not by $\times\mathsf{A}_1$.

It is claimed [19] that the average value should be $\gamma \approx 4/5$. This observation was based on tests which could be blurred by the $\sigma\mathsf{A}$. However, for practical purposes, such results are sufficient because $\times\mathsf{A}$ has been shown to be dominant over $\sigma\mathsf{A}$ in highly overconsolidated clays [19] as well as in

plates and laterally by cutting the membrane. Similar tests in-situ can use cross-hole or down-hole measurements but they can be blurred by the $\sigma\mathsf{A}$ due to the K_0-stress state.

kaolin [9]. Unfortunately, only a few tests from [19] were carried out under hydrostatic stress. In consequence, not much usable data can be found. However, some results from London Clay and Gault Clay referred to in [30] confirmed the discrepancies from $\gamma = 1/2$ and speak for $\times\mathsf{A}_2$ rather than for $\times\mathsf{A}_1$. The exponent $\gamma = 1/2$ was estimated for Bangkok Clay under isotropic stress [26]. Measured values of γ are presented for different αs in Fig. 10.

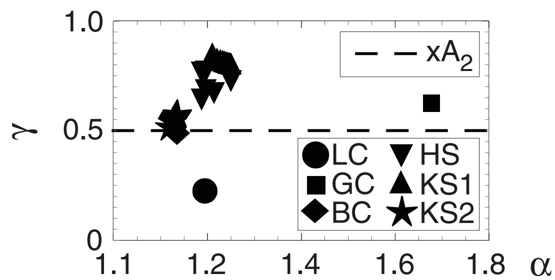

Figure 10: *Parameters γ and α for London Clay (LC) [30], Gault Clay (GC) [30], Bangkok Clay (BC), [26] Hostun Sand (HS) [27] and Kenya Sand (KS1, KS2) [8]*

Some dynamic test data for Kenya Sand [8] and Hostun Sand [27] at different isotropic stress levels, p, revealed an influence of p on the parameter β. This strange effect can be attributed to errors in measurements or to partial destruction of $\times\mathsf{A}$ by isotropic loading. Tests with temporary overloading (up to a high p and back) could help to confirm such a degradation. The dynamic tests prove $\gamma \geq 1/2$ for sands.

Parameter β and the ratio β/γ are plotted as functions of α in Figs. 11 and 12, respectively. The ratio $\beta/\gamma = 2$ was assumed in $\times\mathsf{A}_2$ because of the mathematical convenience. Due to the scatter of experimental data, one can neither confirm nor reject this assumption.

10 Graphic representation of anisotropy

For constitutive rate-type models in the form of an isotropic function $\dot{\boldsymbol{\sigma}}(\boldsymbol{\sigma}^0, \dot{\boldsymbol{\varepsilon}})$, the well known concept [11] of response envelopes can be used for the graphic representation of stiffness. The 2D plots of response envelopes to strain

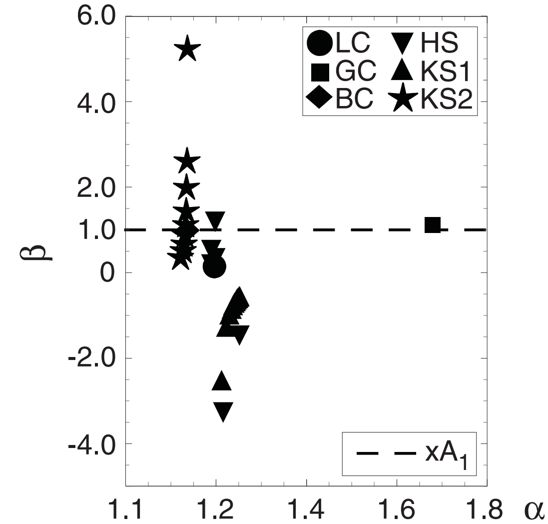

Figure 11: *Parameter β does not correlate with α.*

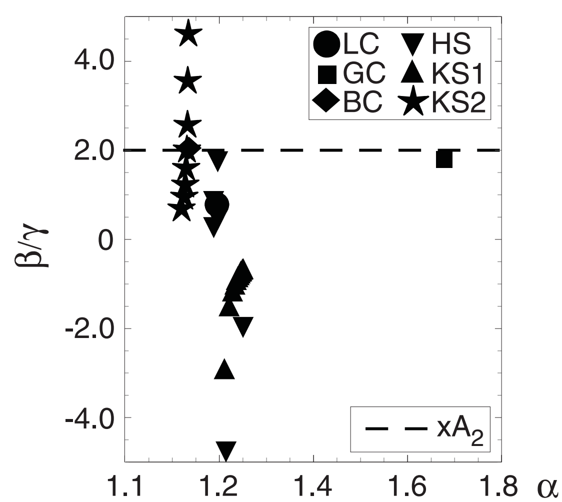

Figure 12: *Ratio β/γ does not correlate with α.*

disturbances require that the initial stress, $\boldsymbol{\sigma}^0$, and all strain rates, $\dot{\boldsymbol{\varepsilon}}$, are *co-axisymmetric*, i.e. axisymmetric with respect to the same symmetry axis.

In the case of $\times\mathsf{A}$, the sedimentation dyad, $\mathbf{M} = \mathbf{m}\,\mathbf{m}$, appears as an additional argument in $\dot{\boldsymbol{\sigma}}(\boldsymbol{\sigma}^0, \dot{\boldsymbol{\varepsilon}}, \mathbf{M})$. This dyad needs not be co-axisymmetric with $\boldsymbol{\sigma}^0$ and $\dot{\boldsymbol{\varepsilon}}$. In such case, the usual 2D response envelopes cannot be plotted, if $\times\mathsf{A}$ spoils the co-axisymmetry of $\boldsymbol{\sigma}^0$ and $\dot{\boldsymbol{\sigma}}$.

For a general graphic representation of stiffness with any $\times\mathsf{A}$, the original concept [11] can be extended. In this extension, the stress increments[18], $\Delta\boldsymbol{\sigma}$, need not be co-axisymmetric with $\boldsymbol{\sigma}^0$.

10.1 2D response envelopes

A response envelope is a polar representation of a tangential stiffness at a given stress $\boldsymbol{\sigma}^0$. Starting from a diagonal and axisymmetric initial stress, $\boldsymbol{\sigma}^0 = \operatorname{diag}(\sigma_1^0, \sigma_2^0, \sigma_3^0)$ with $\sigma_2^0 = \sigma_3^0$, different axisymmetric strain increments of constant length,

$$\begin{gathered}\Delta\boldsymbol{\varepsilon} = r\ \operatorname{diag}\left(\sin\phi, \frac{1}{\sqrt{2}}\cos\phi, \frac{1}{\sqrt{2}}\cos\phi\right) \\ \text{with}\quad r = \text{const} \approx 0.0001 \quad \text{and} \quad 0 \le \phi < 2\pi,\end{gathered} \tag{63}$$

are applied, Fig. 13a. The envelope of the corresponding stress increments, $\Delta\boldsymbol{\sigma} = \Delta\boldsymbol{\sigma}(\phi)$, is termed the response envelope. Linear elasticity maps a circle (63) in the strain space to an ellipse in the stress space, Fig. 13c. Increments $\Delta\boldsymbol{\sigma}$ are co-axisymmetric with $\boldsymbol{\sigma}^0$, if $\boldsymbol{\sigma}^0$ is co-axisymmetric with $\Delta\boldsymbol{\varepsilon}$ and $\times\mathsf{A}$ is absent or its $\mathbf{m}$ is parallel to the symmetry axis. In such cases, the end-stresses, $\boldsymbol{\sigma}^0 + \Delta\boldsymbol{\sigma}$, can be plotted. These plots are quite common in the geotechnical literature. Usually, they are shown on the Rendulić plane, $\sqrt{2}\sigma_r - \sigma_a$, or on the plane of isometric Roscoe invariants, $P - Q$.

Generally, $\boldsymbol{\sigma}^0 + \Delta\boldsymbol{\sigma}$ cannot be plotted because the $\times\mathsf{A}$ may spoil the co-axisymmetry between $\Delta\boldsymbol{\sigma}$ and $\boldsymbol{\sigma}^0$. However, all $\Delta\boldsymbol{\sigma}$ are coplanar, if all $\Delta\boldsymbol{\varepsilon}$ are and because the constitutive relation, $\dot{\boldsymbol{\sigma}}(\boldsymbol{\sigma}^0, \dot{\boldsymbol{\varepsilon}}, \mathbf{M}) = \mathsf{E}(\boldsymbol{\sigma}^0, \mathbf{M}) : \dot{\boldsymbol{\varepsilon}}$, is incrementally linear. Let the following orthogonal strain increments:

- isotropic $\quad \Delta\boldsymbol{\varepsilon}_P = r\ \operatorname{diag}(1, 1, 1)/\sqrt{3}$
- deviatoric axisymmetric $\quad \Delta\boldsymbol{\varepsilon}_Q = r\ \operatorname{diag}(2, -1, -1)/\sqrt{6}$

[18] obtained from strain increments $\Delta\boldsymbol{\varepsilon}$ of equal length and co-axisymmetric with the initial stress $\boldsymbol{\sigma}^0$

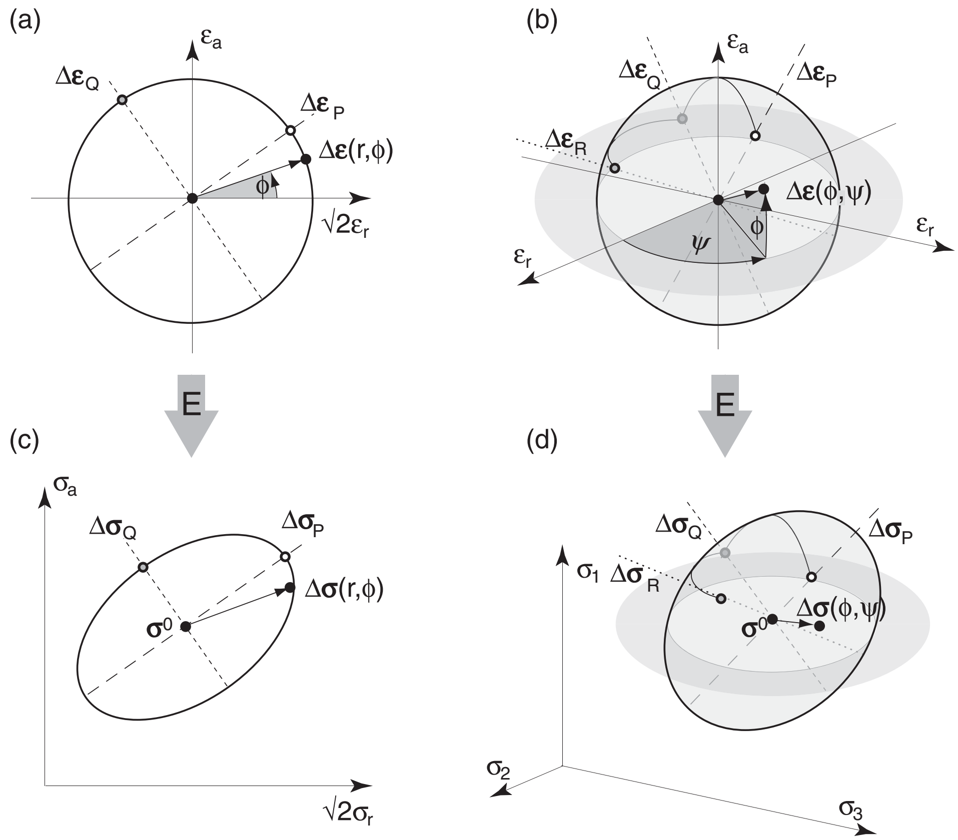

Figure 13: *Isotropic elastic relation* $\dot{\boldsymbol{\sigma}}(\boldsymbol{\sigma}^0, \dot{\boldsymbol{\varepsilon}})$*:*
a) axisymmetric $\boldsymbol{\sigma}^0$ *and co-axisymmetric strain increments* $\Delta\boldsymbol{\varepsilon}$
b) diagonal $\boldsymbol{\sigma}^0$ *and coaxial* $\Delta\boldsymbol{\varepsilon}$
c) stress response $\Delta\boldsymbol{\sigma}$ *for (a)*
d) stress response $\Delta\boldsymbol{\sigma}$ *for (b)*

along $\phi = \phi_P = \arcsin\left(1/\sqrt{3}\right)$ and $\phi = \phi_Q = \arccos\left(1/\sqrt{3}\right)$ produce stress increments, $\Delta\boldsymbol{\sigma}_P$ and $\Delta\boldsymbol{\sigma}_Q$, respectively. These two increments span a plane in 6D stress space. All other stress responses lie in this plane due to the linearity of E. In other words, any response is a linear combination of $\Delta\boldsymbol{\sigma}_P$ and $\Delta\boldsymbol{\sigma}_Q$. After orthonormalization of $\Delta\boldsymbol{\sigma}_P$ and $\Delta\boldsymbol{\sigma}_Q$, they constitute the orthogonal basis $\{\mathbf{e}^\star_P, \mathbf{e}^\star_Q\}$ on the response plane and we may introduce the coordinates, $\Delta P^\star$ and $\Delta Q^\star$, on this plane. Any stress response can be represented as

$$\Delta\boldsymbol{\sigma}(\phi) = \Delta P^\star \ \mathbf{e}^\star_P + \Delta Q^\star \ \mathbf{e}^\star_Q, \tag{64}$$

for example $\Delta\boldsymbol{\sigma}(\phi_P) = \Delta P^\star \ \mathbf{e}^\star_P$.

10.2 An example of 2D response

Experiments on kaolin [9] show that the effects from $\times\mathsf{A}$ dominate over the ones from $\sigma\mathsf{A}$, Fig. 3. It turns out that, for kaolin, the $\times\mathsf{A}_1$ with a single anisotropy parameter α simulates the experiments sufficiently well and β is not necessary. In sedimentary clays, however, $\times\mathsf{A}_1$ can be inaccurate, see Section 9. As an example, 2D response envelopes from the superposition of $\sigma\mathsf{A}$ from (14) and $\times\mathsf{A}_2$ are plotted in the $\Delta P^\star - \Delta Q^\star$ plane in Fig. 14.

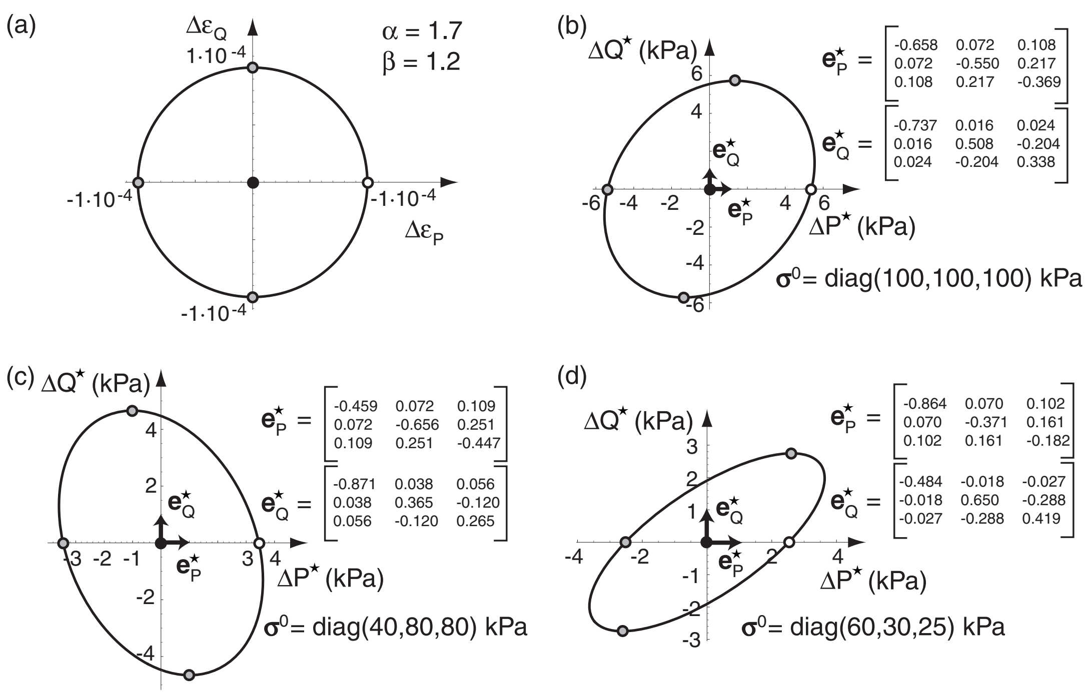

Figure 14: *Cross-anisotropic elastic relation* $\dot{\boldsymbol{\sigma}}(\boldsymbol{\sigma}^0, \dot{\varepsilon}, \mathbf{M})$ *with* $\sigma\mathsf{A}$ *from (14) and with* $\times\mathsf{A}_2$*: 2D isometric stress plots (b,c,d) were calculated at different diagonal initial stresses* $\boldsymbol{\sigma}^0$ *and for the same sedimentation* $\mathbf{m} = \{1, 2, 3\}^{\rightarrow}$.

10.3 3D response envelopes

To plot 3D response envelopes, solely the coaxiality of $\boldsymbol{\sigma}^0$ and $\dot{\boldsymbol{\varepsilon}}$ in $\dot{\boldsymbol{\sigma}}(\boldsymbol{\sigma}^0, \dot{\boldsymbol{\varepsilon}})$ is required. If the $\times\mathsf{A}$ is present, all arguments in $\dot{\boldsymbol{\sigma}}(\boldsymbol{\sigma}^0, \dot{\boldsymbol{\varepsilon}}, \mathbf{M})$ must be coaxial.

Starting from a given initial stress, $\boldsymbol{\sigma}^0 = \operatorname{diag}(\sigma_1^0, \sigma_2^0, \sigma_3^0)$, diagonal, axisymmetric strain increments of constant length,

$$\Delta\boldsymbol{\varepsilon}(\phi, \psi) = r \operatorname{diag}(\sin\phi, \cos\phi\cos\psi, \cos\phi\sin\psi) \quad (65)$$
$$\text{with} \quad r = \text{const} \approx 0.0001 \quad \text{and} \quad 0 \leq \phi, \psi < 2\pi,$$

are applied, Fig. 13b. They can be encompassed by a sphere in the 3D space of principal strains. In the case of a linear elastic constitutive relation, $\dot{\boldsymbol{\sigma}}(\boldsymbol{\sigma}^0, \dot{\boldsymbol{\varepsilon}}) = \mathsf{E}(\boldsymbol{\sigma}^0) : \dot{\boldsymbol{\varepsilon}}$, the end-stresses, $\boldsymbol{\sigma}^0 + \Delta\boldsymbol{\sigma}$, form an ellipsoidal response envelope in the 3D space of principal stresses, Fig. 13d. The respective stress increments, $\Delta\boldsymbol{\sigma} = \Delta\boldsymbol{\sigma}(\phi, \psi)$, are coaxial with $\boldsymbol{\sigma}^0$, if $\boldsymbol{\sigma}^0$ and $\Delta\boldsymbol{\varepsilon}$ are. Generally, the coaxiality of $\boldsymbol{\sigma}^0$ and $\Delta\boldsymbol{\sigma}$ may be violated by the presence of the $\times\mathsf{A}$, when $\mathbf{M}$ is not coaxial with $\boldsymbol{\sigma}^0$.

Similarly as in the 2D case, we define three orthogonal strain increments:

- isotropic $\quad \Delta\boldsymbol{\varepsilon}_P = r \operatorname{diag}(1, 1, 1)/\sqrt{3}$
- deviatoric axisymmetric $\quad \Delta\boldsymbol{\varepsilon}_Q = r \operatorname{diag}(2, -1, -1)/\sqrt{6}$
- deviatoric anti-planar $\quad \Delta\boldsymbol{\varepsilon}_R = r \operatorname{diag}(0, 1, -1)/\sqrt{2}$.

They correspond to the following angles:

- $\phi = \phi_P = \arcsin\left(1/\sqrt{3}\right), \psi = \psi_P = \pi/4$
- $\phi = \phi_Q = \arccos\left(1/\sqrt{3}\right), \psi = \psi_Q = \pi/4$
- $\phi = \phi_R = 0, \psi = \psi_R = 7\pi/4$.

The respective stress increments, $\Delta\boldsymbol{\sigma}_P, \Delta\boldsymbol{\sigma}_Q$ and $\Delta\boldsymbol{\sigma}_R$, are not necessarily orthogonal but they span a 3D subspace of the 6D stress space. Analogously as in the 2D case, these stress increments can be orthonormalized to define the basis $\{\mathbf{e}_P^\star, \mathbf{e}_Q^\star, \mathbf{e}_R^\star\}$ and the coordinate system $\Delta P^\star - \Delta Q^\star - \Delta R^\star$ of this subspace. Due to the incremental linearity, all stress increments can be expressed as linear combinations of the basis tensors,

$$\Delta\boldsymbol{\sigma}(\psi, \phi) = \Delta P^\star \ \mathbf{e}_P^\star + \Delta Q^\star \ \mathbf{e}_Q^\star + \Delta R^\star \ \mathbf{e}_R^\star, \quad (66)$$

for example $\Delta\boldsymbol{\sigma}(\phi_P, \psi_P) = \Delta P^\star \ \mathbf{e}_P^\star$ with $\phi_P = \arcsin(1/\sqrt{3})$ and $\psi_P = \pi/4$.

10.4 An example of 3D response

The 3D stress response envelopes were obtained with the identical constitutive model and the same material constants as for the 2D ones from Fig. 14. The 3D strain increments $\Delta\boldsymbol{\varepsilon}$ were applied to plot $\Delta\boldsymbol{\sigma}$ in $\Delta P^\star - \Delta Q^\star - \Delta R^\star$ system, Fig. 15.

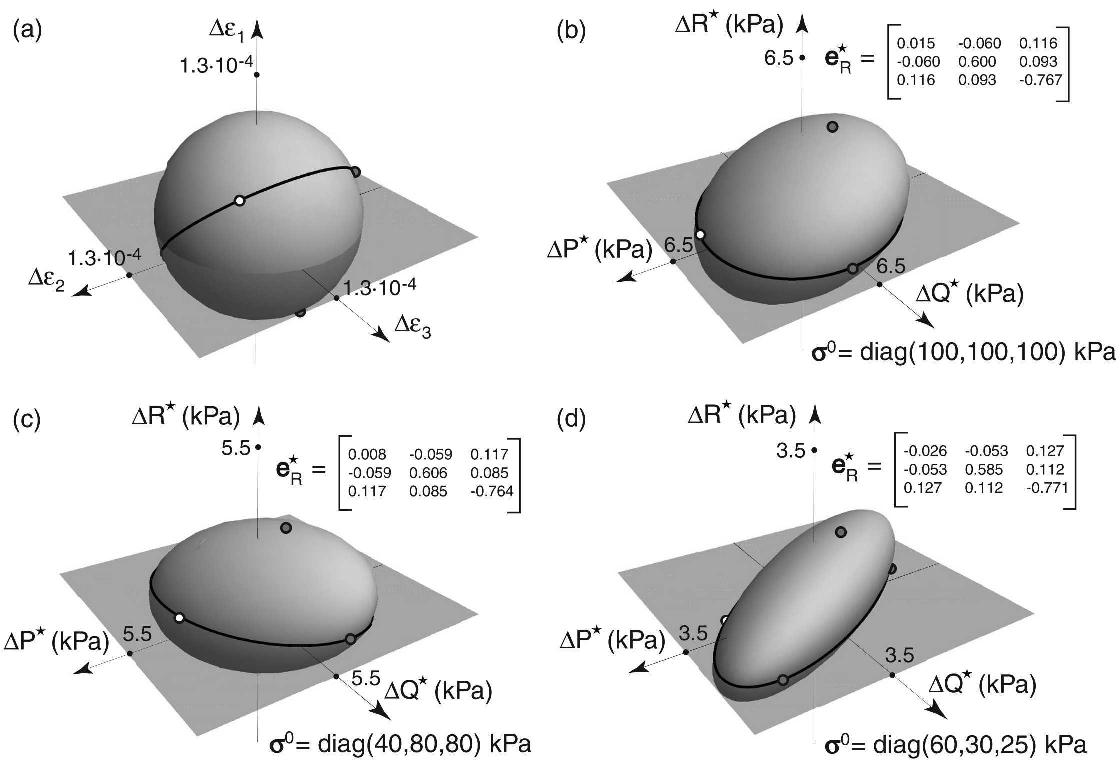

Figure 15: *Cross-anisotropic elastic relation* $\dot{\boldsymbol{\sigma}}(\boldsymbol{\sigma}^0, \dot{\boldsymbol{\varepsilon}}, \mathbf{M})$ *with* $\sigma\mathsf{A}$ *from (14) and* $\times\mathsf{A}_2$*: 3D isometric stress plots (b,c,d) were calculated at different diagonal initial stresses* $\boldsymbol{\sigma}^0$ *and for the same sedimentation* $\mathbf{m} = \{1, 2, 3\}^{\to}$.

10.5 Polar diagrams of wave velocity

Using the acoustic tensor $\mathbf{\Gamma}$ from (58), the velocities v of different waves can be plotted as functions of the direction of propagation $\mathbf{n}$. The directional dependence of wave velocities can be then visualized in the form of polar diagrams for each wave type.

An example of polar diagrams obtained with the superposition of $\times\mathsf{A}_2$ and $\sigma\mathsf{A}$ from (13) is shown in Fig. 16.

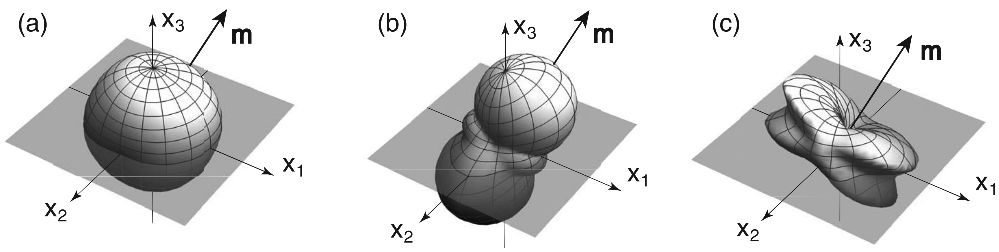

Figure 16: *Polar diagrams of three wave velocities for an abstract material with* $\times\mathsf{A}_2$

11 Scaling of yield functions

The anisotropy tensor Q from $\times\mathsf{A}_1$ and $\times\mathsf{A}_2$ may have a variety of applications beyond elasticity. A yield stress criterion describes the boundary of all accessible stress states, $F(\boldsymbol{\sigma}) \leq 0$, where $F(\boldsymbol{\sigma})$ is an isotropic function of stress. For example, Matsuoka and Nakai [18] proposed the following yield function

$$F(\boldsymbol{\sigma}) \equiv \operatorname{tr}\boldsymbol{\sigma}\operatorname{tr}\left(\boldsymbol{\sigma}^{-1}\right) - 8\tan^2\varphi - 9, \tag{67}$$

wherein φ is the friction angle.

The $\times\mathsf{A}$ can be imposed to stress using the anisotropy tensor from (32) and substituted into $F(\boldsymbol{\sigma})$, i.e. $F^{\times\mathsf{A}2}(\sigma_{ab}) = F(Q_{abcd}\sigma_{cd})$. As an example, $F(\boldsymbol{\sigma})$ from (67) with the $\times\mathsf{A}_2$ was plotted in the deviatoric plane, Fig. 17. The transformed yield function $F^{\times\mathsf{A}2}(\boldsymbol{\sigma})$ requires calibration of the corresponding friction angle $\varphi^{\times\mathsf{A}2}$.

In the literature, one may find some attempts to make a yield surface $F(\boldsymbol{\sigma})$ cross-anisotropic, e.g. [16]. In comparison, scaling with the anisotropy tensor, Q, is an elegant and easy method.

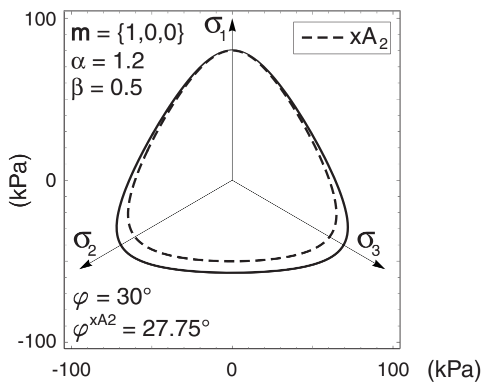

Figure 17: *Anisotropic (dashed) yield function obtained from isotropic (solid) one using* $\times\mathsf{A}_2$

12 Summary

Inherent cross-anisotropy and stress-induced anisotropy, can be easily superposed within the elastic range, in particular dealing with geotechnical (barotropic) elastic potentials. The pure anisotropy tensor, Q, depends on the sedimentation direction, $\mathbf{m}$, and some material constants. The simplified versions, $\times\mathsf{A}_1$ and $\times\mathsf{A}_2$, of cross-anisotropy could be used to build such Q but not the general form, $\times\mathsf{A}_3$. The proposed pure anisotropy does not violate the Second Law, if superposed with hyperelasticity. The pure anisotropy can be applied also to any isotropic potential function, for example to a yield surface.

The proposed calibration procedure for Q can be based on static, cyclic or dynamic tests. The popular concept of response envelopes [11] has been extended to provide the graphic representation of polar stiffness at presence of $\times\mathsf{A}$. For this purpose, a new isometric representation system has been proposed. The concept of pure anisotropy has been compared to some recent approaches from the literature. Visualization of the superposed $\times\mathsf{A}_2$ and $\sigma\mathsf{A}$ conducted with the algebra program MATHEMATICA has been given in examples. All notebooks and packages involved in this paper are available from the authors.

13 Appendices

A Static calibration for $\times\mathsf{A}_1$

The parameters of $\times\mathsf{A}_1$ have been found from (52,53) for *undrained* triaxial tests in the static calibration

$$\alpha = \frac{a+\sqrt{a^2+12r\,b}}{b} \quad \text{and} \quad \nu_h = \frac{2a}{9\eta_v(r-4)+\sqrt{a^2+12r\,b}-12} \tag{68}$$

with abbreviations $a = 3\eta_v(r-4)+4(r-1)$ and $b = 2(3\eta_v-2)(r-4)$. Given α and ν_h from (68), one may use (56) to obtain

$$E_v \quad = \quad \frac{\dot{\sigma}_{av}^{\text{tot}}}{\dot{\varepsilon}_{av}} s \quad \text{with} \quad s = \frac{2(\nu_h+1)(1-2\nu_h)}{2+\alpha^2-4\alpha\nu_h-2\nu_h}\,. \tag{69}$$

These parameters can also be found from the system (57) for static, *drained* triaxial tests and it follows that

$$\alpha = \frac{1}{2}(-1+c_1/c_2) \quad \text{and} \quad \nu_h = \frac{1}{4}(-1+r_v+c_1c_2) \quad \text{and} \quad E_v = \frac{\dot{\sigma}_{av}}{\dot{\varepsilon}_{av}} \tag{70}$$

with abbreviations $c_1 = \sqrt{1-r_v}$, $c_2 = \sqrt{9-8r_h-r_v}$, $r_v = \dot{\varepsilon}_{\text{vol}\,v}/\dot{\varepsilon}_{av}$ and $r_h = \dot{\varepsilon}_{\text{vol}\,h}/\dot{\varepsilon}_{ah}$.

B Acoustic tensor for $\times\mathsf{A}_2$

In the general case of $\mathbf{n} = \{n_1, n_2, n_3\}$ with $\mathsf{E}^{\times\mathsf{A}2}$ after (31) and $\mathbf{m} = \{0,0,1\}$, the acoustic tensor has the following form

$$\mathbf{\Gamma} = E \begin{bmatrix} \frac{\Omega^2\left[\alpha n_2^2 A + n_3^2 A + \alpha n_1^2(\nu-1)B\right]}{\alpha AB} & \frac{\Omega^2 n_1 n_2(A-\nu B)}{AB} & \frac{\Omega n_1 n_3(\Omega A-\alpha B)}{\alpha AB} \\ \frac{\Omega^2 n_1 n_2(A-\nu B)}{AB} & \frac{\Omega^2\left[\alpha n_1^2 A + n_3^2 A + \alpha n_2^2(\nu-1)B\right]}{\alpha AB} & \frac{\Omega n_2 n_3(\Omega A-\alpha B)}{\alpha AB} \\ \frac{\Omega n_1 n_3(\Omega A-\alpha B)}{\alpha AB} & \frac{\Omega n_2 n_3(\Omega A-\alpha B)}{\alpha AB} & \frac{n_3^2(\nu-1)}{A} + \frac{\Omega^2\left(n_1^2+n_2^2\right)}{\alpha B} \end{bmatrix}, \tag{71}$$

wherein $E = E_v$, $\nu = \nu_h$, $A = 2\nu^2+\nu-1$, $B = 2(\nu+1)$ and $\Omega = \alpha^{1/\beta}$. For horizontal and vertical waves, one obtains two special cases,

$$\mathbf{\Gamma} \overset{\mathbf{n}\perp\mathbf{m}}{=} E \begin{bmatrix} \frac{\Omega^2(\nu-1)}{A} & 0 & 0 \\ 0 & \frac{\Omega^2}{B} & 0 \\ 0 & 0 & \frac{\Omega^2}{\alpha B} \end{bmatrix} \quad \text{and} \quad \mathbf{\Gamma} \overset{\mathbf{n}\parallel\mathbf{m}}{=} E \begin{bmatrix} \frac{\Omega^2}{\alpha B} & 0 & 0 \\ 0 & \frac{\Omega^2}{\alpha B} & 0 \\ 0 & 0 & \frac{\nu-1}{A} \end{bmatrix}, \tag{72}$$

and set of equations (60) can be determined from the eigenvalues of $\mathbf{\Gamma}$.

Let us define three of polarization cosines $\Pi_i = \mathbf{n} \cdot \vec{\mathbf{A}}_i$. In the case of isotropic elasticity, $\mathbf{\Pi} = \{1, 0, 0\}$ means one P- and two S-waves. At presence of $\times\mathsf{A}_2$, one can speak of only one S-wave[19]. Its polarization is perpendicular to both $\mathbf{n}$ and $\mathbf{m}$. Two other waves lie in the plane spanned by $\mathbf{n}$ and $\mathbf{m}$. All three wave velocities are different. For example, $\alpha = 1.8$ and $\beta = 1.2$ in $\times\mathsf{A}_2$ with $\mathbf{n} = \{1, 2, 3\}^{\rightarrow}$ yield $\mathbf{\Pi} = \{0.94, 0, 0.33\}$, wherein the second polarization corresponds to the S-wave. The other two polarizations depend on α, β and on the angle between $\mathbf{n}$ and $\mathbf{m}$.

Declarations

Funding

Not applicable

Conflicts of interest/Competing interests

Not applicable

Availability of data and material

All data was digitalized from the figures published in literature.

Code availability

The relevant packages and notebooks for the algebra program MATHEMATICA are available from the authors.

Authors' contributions

Not applicable

[19]except for the special cases $\mathbf{n} \| \mathbf{m}$ and $\mathbf{n} \perp \mathbf{m}$

References

[1] A. Amorosi, F. Rollo, and G. T. Houlsby. A nonlinear anisotropic hyperelastic formulation for granular materials: comparison with existing models and validation. *Acta Geotechnica*, 15(1):179–196, 2020. 2.1

[2] Z.P. Bažant. *Stability of structures*. Oxford University Press, New York, Oxford, 1991. 1

[3] J.P. Boehler and A. Sawczuk. On yielding of oriented solids. *Acta Mechanica*, 27:185–206, 1977. 7

[4] I.R. Borja, C. Tamagnini, and A. Amorosi. Coupling plasticity and energy-conservating elasticity models for clays. *Journal of Geotechechnical Geoenvironmental Engineering, ASCE*, 123(10):948–957, 1997. 2.1

[5] H.R. Boyce. A non-linear model for the elastic behaviour of granular materials under repeated loading. pages 285–294, 1980. Proceedings of Int. Symp. on Soils under Cyclic and Transient Loading, Swansea. 2.1

[6] P. Chadwick and G. D. Smith. *Advances in Applied Mechanics*, volume 17, chapter Foundations of the Theory of Surface Waves in Anisotropic Elastic Materials. School of Mathematics and Physics University of East Anglia Norwich, England, 1977. 8.2

[7] M. Cudny and K.. Staszewska. A hyperelastic model for soils with stress-induced and inherent anisotropy. *Acta Geotechnica*, 2021. 2.1

[8] V. Fioravante, D. Giretti, and M. Jamiolkowski. Small strain stiffness of carbonate Kenya Sand. *Engineering Geology*, 161:65–80, 2013. 1, 6, 8.2, 10, 9

[9] S. Gehring. Fortgesetzte Untersuchungen zur hyperelastischen Steifigkeit von Ton. Master's thesis, Institut für Boden- und Felsmechanik, Karlsruher Institut für Technologie, April 2020. 2.1, 2.1, 2.1, 3, 5, 9, 10.2

[10] J. Graham and G. T. Houlsby. Anisotropic elasticity of natural clay. *Géotechnique*, 33(2):165–180, 1983. 5, 5, 5

[11] G. Gudehus. A comparison of some constitutive laws for soils under radially symmetric loading and unloading. In *Proceedings of the 3rd International Conference On Numerical Methods in Geomechanics, Aachen*, Aachen, 1979. Balkema. 1, 2.1, 10, 12

[12] G. T. Houlsby, A. Amorosi, and F. Rollo. Non-linear anisotropic hyperelasticity for granular materials. *Computers and Geotechnics*, 115:1–11, 2019. 2.1

[13] G.T. Houlsby and A.M. Puzrin. *Principles of Hyperplasticity*. Springer, London, 2006. 1

[14] L. Knittel, T. Wichtmann, A. Niemunis, G. Huber, E. Espino, and T. Triantafyllidis. Pure elastic stiffness of sand represented by response envelopes derived from cyclic triaxial tests with local strain measurements. *Acta Geotechnica*, 2020. DOI: 10.1017/S0962492904000212. 2.1

[15] L.J. Knittel. Fortgesetzte quasi-statische Untersuchungen zur Elastizität von Sand als Grundlage eines neuen hypoplastischen Stoffmodells. Master's thesis, Institut für Boden- und Felsmechanik, Karlsruher Institut für Technologie, September 2014. 2.1, 2

[16] Y. Kong, J. Zhao, and Y. Yao. A failure criterion for cross-anisotropic soils considering microstructure. *Acta Geotechnica*, 8:665–673, 2013. 11

[17] A. S. Lodge. The transformation to isotropic form of the equilibrium equations for a class of anisotropic elastic solids. *The Quarterly Journal of Mechanics and Applied Mathematics*, 8(2):211–225, 1955. 3, 6

[18] H. Matsuoka and T. Nakai. A new failure for soils in three-dimensional stresses. In *Deformation and Failure of Granular Materials*, pages 253–263, 1982. Proc. IUTAM Symp. in Delft. 11

[19] D. Mašín and J. Rott. Small strain stiffness anisotropy of natural sedimentary clays: review and a model. *Acta Geotechnica*, 9:299–312, 2014. 5, 6, 9

[20] A. Niemunis and M. Cudny. On hyperplasticity for clays. *Computers and Geotechnics*, 23:221–236, 1998. 2.1, 2.1

[21] A. Niemunis, C.E. Grandas Tavera, and T Wichtmann. Peak Stress Obliquity in drained and undrained sands. Simulations with Neohypoplasticity. In Th. Triantafyllidis, editor, *Holistic simulation of geotechnical installation processes. Numerical and physical modelling.* , volume 80, pages 85–114. Springer, 2016. 2.1, 5

[22] A. Niemunis and L. Knittel. Removal of the membranepenetration error from triaxialdata. *Open Geomechanics*, SSN: 2644-9676:article no. 5, 2020. DOI: https://doi.org/10.5802/ogeo.7. 8.1

[23] A. Niemunis, L. F. Prada-Sarmiento, and C. E. Grandas-Tavera. Paraelasticity. *Acta Geotechnica*, 6(2):67–80, 2011. 1

[24] A. Niemunis, T. Wichtmann, and T. Triantafyllidis. A high-cycle accumulation model for sand. *Computers and Geotechnics*, 32(4):245–263, 2005. 1

[25] V. A. Osinov and Wu W. Simple shear in sand with an anisotropic hypoplastic model. *Geomechanics and Geoeingineering*, 1:43–50, 2006. 5, 3, 3

[26] W. Ratananikoma, S. Likitlersuanga, and S. Yimsiri. An investigation of anisotropic elastic parameters of bangkok clay from vertical and horizontal cut specimens. *Geomechanics and Geoengineering: An International Journal*, 8:15–27, 2013. 9, 10

[27] T. Sadek, M. Lings, L. Dihoru, and D. Muir-Wood. Wave transmission in Hostun sand: multiaxial experiments. *Rivista Italiana Di Geotechnica*, (2):69–84, 2007. 1, 8.2, 10, 9

[28] P. Vermeer. A five-constant model unifying well established concepts. In *Constit. Relat. for Soils*, pages 175–198. Balkema, Holland, 1982. Proceedings of the International Workshop in Grenoble. 2.1

[29] T. Wichtmann. Karlsruhe kaolin database @ONLINE. 8.1, 6

[30] S. Yimsiri and K. Soga. Cross-anisotropic elastic parameters of two natural stiff clays. *Géotechnique*, 61(9):809–814, 2011. 9, 10

[31] M. Zytynski, M.F. Randolph, R. Nova, and C.P. Wroth. On modelling the unloading-reloading behaviour of soils. *International Journal for Numerical and Analytical Methods in Geomechanics*, 2:87–94, 1978. 1